BOREAS An international journal of Quaternary research

Glukhoye Lake: Middle to Late Holocene environments of Kunashir Island (Kuril Archipelago, Russian Far East)

ANATOLY V. LOZHKIN, MARINA V. CHEREPANOVA, PATRICIA M. ANDERSON, PAVEL S. MINYUK AND BRUCE P. FINNEY

BOREAS

Lozhkin, A. V., Cherepanova, M. V., Anderson, P. M., Minyuk, P. S. & Finney, B. P.: Glukhoye Lake: Middle to Late Holocene environments of Kunashir Island (Kuril Archipelago, Russian Far East). *Boreas.* https://doi.org/10.1111/bor.12565. ISSN 0300-9483.

A multiproxy analysis of a sediment core from Glukhoye Lake in the southern Kuril Islands indicates that the basin originated *c*. 8.2 cal. ka BP as a brackish lagoon with the subsequent development of a freshwater lake (*c*. 4.0 to 3.3 cal. ka BP), a bog (*c*. 3.3 to 2.4 cal. ka BP) and a second lake (*c*. 2.4 cal. ka BP to present). The basin history primarily reflects local coastal dynamics and is not related to proposed Archipelago-wide changes in sea level. Between *c*. 8.2 and 8.0 cal. ka BP, the vegetation of southern Kunashir Island was characterized by *Betula–Quercus* forest with a secondary component of temperate broadleaf trees. *Quercus* broadleaf forest established *c*. 8.0 to 6.5 cal. ka BP and represents the Holocene thermal maximum. The remainder of the record shows a gradual decrease in temperate and an increase in conifer taxa, indicating a gradual cooling from the Holocene thermal maximum to *c*. 2.3 cal. ka BP. Maxima in *Picea* and *Abies* pollen between *c*. 2.3 and 1.1 cal. ka BP suggest conditions that were slightly cooler than present. Palaeovegetation changes in the Kuril Islands as inferred from lake and section data differ in the timing and/or composition of the vegetation communities, although results from the two types of sites become more similar as the number of sections increases. The lake results do not support a previous conceptual model developed for the southern Russian Far East, which linked changes in sea levels to Holocene climate fluctuations. Rather the depositional environments in the lake cores seem more related to coastal dynamics that are independent of fluctuations in sea levels or climate. The difficulty in developing accurate age models for sites with multiple depositional environments may be the most important obstacle for documenting and understanding the Archipelago's vegetation and climate histories.

Anatoly V. Lozhkin and Pavel S. Minyuk, North East Interdisciplinary Science Research Institute N.A. Shilo, Far East Branch, Russian Academy of Sciences, Magadan, Russia 68500; Marina V. Cherepanova, Federal Scientific Center of East Asian Terrestrial Biodiversity, Far East Branch, Russian Academy of Sciences, Vladivostok, Russia 690022; Patricia M. Anderson (corresponding author: pata@uw.edu), Earth and Space Sciences and Quaternary Research Center, University of Washington, Seattle, WA 98195-1310, USA; Bruce P. Finney, Departments of Biological Sciences and Geosciences, Idaho State University, Pocatello, ID 83209, USA; *received 18th May 2021, accepted 15th September 2021.*

The Kuril Archipelago, spanning ~1200 km between the Kamchatka Peninsula of northeastern Russia and Hokkaido Island of northern Japan (Fig. 1A), encompasses the northern Circumboreal and southern East Asian floristic zones (Pietsch *et al*. 2003). Located on the eastern edge of the southern Russian Far East (SRFE), the islands lay within a tectonic convergence zone, resulting in a long history of intensive volcanic and seismic activity (Bourgeois *et al*. 2006). Today ~160 volcanos are found in the Kurils, of which 40 are still active (Pietsch *et al*. 2003). The island chain separates the relatively warmer Okhotsk Sea from the cool North Pacific Ocean (Gorbarenko *et al*. 2014; Fig. 1B). Additionally, the Soya Current brings warmer waters from the Japan Sea to the Okhotsk Sea, thereby ameliorating conditions on the western shores of the southern Kurils. The regional climate of the Archipelago is formed by the interaction of the Siberian High and Aleutian Low in winter and the Asiatic Low and the North Pacific High in summer (Martyn 1992; Mock 2002). Additionally, the SRFE is located at the northeastern limit of the modern East Asian Monsoon (Ding & Chan 2005).

This suite of geological, oceanic and atmospheric influences illustrates the range of factors that have shaped the landscapes and climates of the Kuril Islands. The temporal and spatial scales of these factors, as represented in the palaeorecords, also vary greatly from local, short-term events (e.g. volcanic eruptions and tsunamis) to longer, regionwide changes (e.g. atmospheric circulation). Thus, the dynamic geological setting and the Archipelago's position at the intersection of three major atmospheric features make the Kuril Islands a challenging area for unravelling the regional vs. local palaeovegetation patterns and ultimately for describing Holocene climates based on the palaeobotanical data.

Palaeoenvironmental investigations in this intriguing area of northeastern Asia were few (e.g. Pryalukhina 1961; Jouze 1962; Alexsandrova, 1971) prior to the late 20th century, when expeditions led initially by A.M. Korotky (Korotky *et al*. 1988, 1996, 2000; Korotky 2002) and later by N.G. Razjigaeva (Razjigaeva *et al*. 2013 and references therein) provided ground-breaking information on late Quaternary environments of the Archipe-

DOI 10.1111/bor.12565

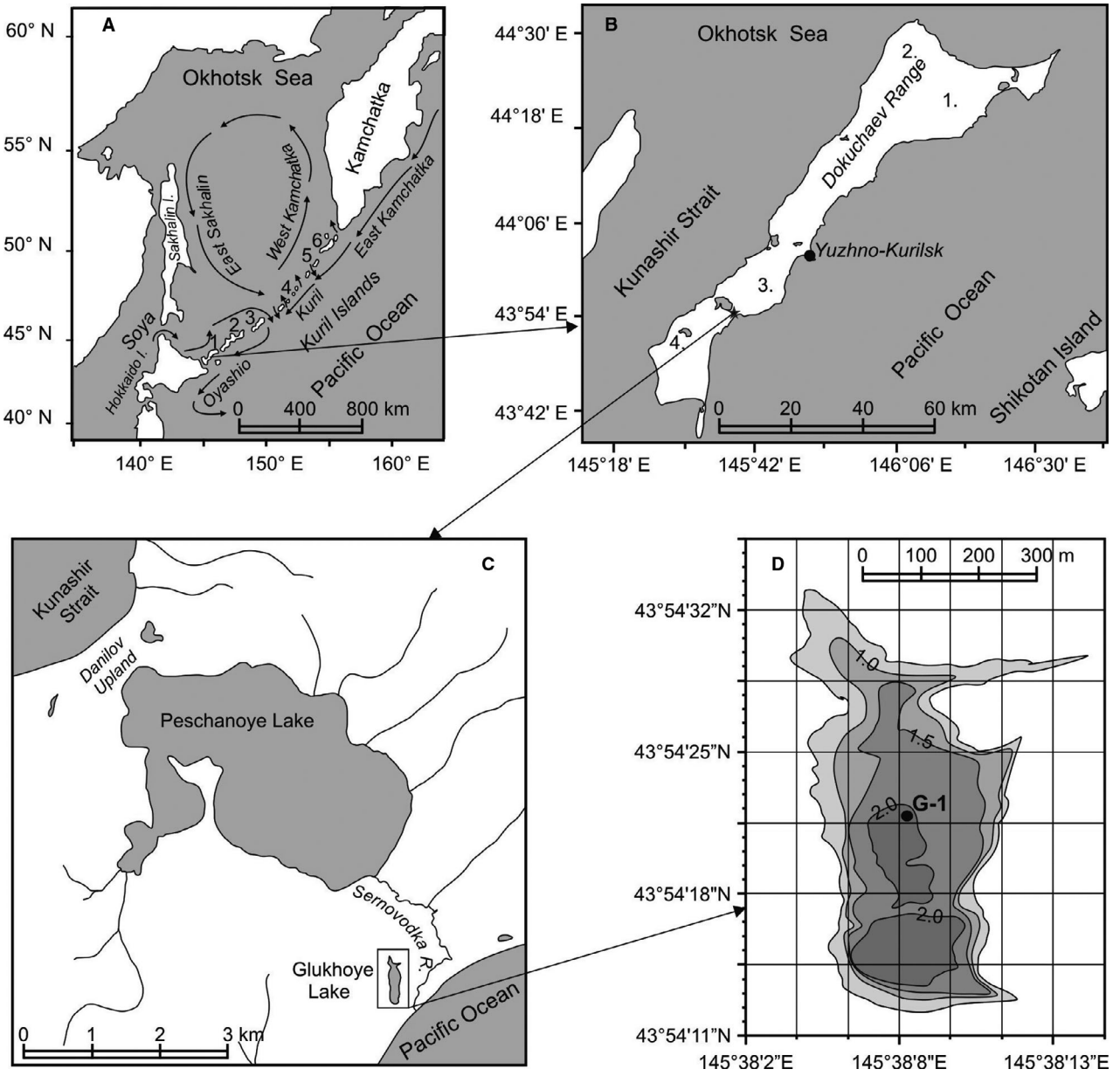

Fig. 1. Maps of the study area. A. Location of the Kuril Islands. Only the Greater Kuril Ridge (Kunashir northward to Paramushir Island) is shown. Sites from the Lesser Kuril Ridge, a set of small islands to the SE of Kunashir Island, are not included in this paper. Arrows indicate locations and directions of marine currents (Gorbarenko *et al*. 2014). Islands mentioned in the text: 1 = Kunashir; 2 = Iturup; 3 = Urup; 4 = Rasshua; 5 = Onekotan; 6 = Paramushir. B. Kunashir Island showing locations for: 1 = Tyatya Volcano (1819 m a.s.l.); 2 = Ruruv Volcano (1484 m a.s.l.); 3 = Mendeleev Volcano (887 m a.s.l.); 4 = Golovnin Volcano (514 m a.s.l.). C. Sernovodsky Isthmus, Kunashir Island. D. Bathymetric map of Glukhoye Lake; G-1 represents the coring location.

lago. Their work with sections from both the Pacific and Okhotsk sides of the islands provided a rich database for inferring past landscape changes, documenting the impact of volcanos and tsunamis on local landscapes and exploring the influences of local vs. regional factors on the palaeoenvironmental record (Razjigaeva *et al*. 2004, 2011a, 2013, 2017). These investigations, when coupled with data from the mainland, also revealed an intriguing and complex climate history, one that was linked closely to sea level changes (Korotky *et al*. 1988, 1996, 2000, 2005; Razjigaeva *et al*. 2004.

While greatly informative, palaeodata from sections have potential shortcomings, particularly in developing reliable age models for sediments with discontinuous depositional histories or using palynological data, which potentially is biased by the input of the local vegetation, to interpret the palaeovegetation or palaeoclimate (Prentice 1988; Davis 2000). Because variations in site

lithologies and vegetation have been used as the main proxies for inferring Holocene climate fluctuations in the Kuril Islands (e.g. Korotky *et al*. 1996; Razjigaeva *et al*. 2004), a further evaluation of the section data as applied to broader trends in past vegetation and ultimately in the palaeoclimate seems appropriate. To that end, a north–south transect of lakes was sampled as part of the Kuril Islands Biocomplexity Project with the goals of (i) improving the understanding of the nature and chronology of events that shaped the Holocene landscapes of the Kuril Islands through the multiproxy analyses of lacustrine records and (ii) assessing whether the Kuril vegetation and depositional histories in this geologically dynamic region were primarily influenced by local factors (e.g. local changes in coastal dynamics; impact of volcanic eruptions on local vegetation) or whether more regional signals have been preserved in the palaeorecords. Our discussion focuses on the Greater Kuril Ridge, composed of Kunashir through Paramushir Islands (Fig. 1A), and does not include the Lesser Kuriles, a group of six islands which are located ~75 km to the east of Kunashir Island (see Razjigaeva *et al*. 2008 for a discussion of the environmental history of this smaller group of islands).

In this paper, we report on a multiproxy study of sediments from Glukhoye Lake, southeastern Kunashir Island (43°54′ 25″N 145°38′ 8″E; ~4 m a.s.l., Fig. 1B, C). It is the last of the lacustrine cores analysed for the Biocomplexity Project (note: we refer to sites that are currently freshwater basins as 'lakes', even though other depositional environments characterized the site in the past). We explore the evolution of the Glukhoye basin, and as with the other lake records (Lozhkin *et al*. 2010, 2017, 2020; Anderson *et al*. 2015), we evaluate the potential influence of local depositional factors on the palynological record. We then consider the suitability of lacustrine and non-lacustrine records for use in defining local vs. regional vegetation patterns and the relationship of changes in vegetation, climate and sea levels in the Greater Kuril Ridge during the Middle and Late Holocene.

Study area

Kunashir Island

Kunashir Island is the southernmost island in the Kuril Archipelago (Fig. 1A). It is ~123-km long and varies between 4 and 30 km in width (Goldfarb 2014). The north–south trending Dokuchaev Range (Fig. 1B), which was formed by eruptive craters and their ejecta (Kotlyakov *et al*. 2009; Ganzei 2011), is the island's main topographic feature. To the south of Mendeleev Volcano, a broad lowland dominates the Okhotsk side and central areas of the island (elevations generally <100 m a.s.l.). Within this lowland, the Sernovodsky Isthmus cross-cuts Kunashir from east to west (Fig. 1C). The isthmus is mostly occupied by Peschanoye Lake and otherwise is characterized by boggy landscapes. Volcanic terrain is found on the southeastern coast dominated by the presence of Golovnin Volcano.

The bedrock geology of Kunashir Island reflects a relatively young history dominated by volcanic activity and marine, riverine and aeolian processes (Kotlyakov *et al*. 2009). The bedrock includes two Neogene suites characterized by volcanic and sedimentary rocks. Poorly defined Quaternary deposits (e.g. alluvium, slope deposits, marine, lacustrine, peats, aeolian sand, gravels, boulders) overlie the volcanic material. The south-central island is characterized by Quaternary sediments, which are similar to deposits found in the north. Palaeotsunami deposits extend up to 1 km inland on the Pacific side of the island, with a splash height of up to ~7 m. These deposits are dated to 1.0, 1.4 to 1.6, 1.7 to 1.8 and 2.0 to 2.1 cal. ka BP and appear to be associated with strong earthquakes (Razjigaeva *et al*. 2017).

Meteorological data from Yuzhno–Kurilsk (Fig. 1B) indicate mean annual, January and July temperatures of 5.0, −4.6 and 12.5 °C, respectively, with the warmest conditions in August (15.8°C; http://climatebase.ru/station/32165). Mean annual, January and July precipitation values are 1245.2, 58.8 and 126.6 mm, with September being the wettest month (171.1 mm). Kunashir experiences distinctive cold (January to March, −6.0 to −3.2 °C), warm (July to September 12.615.8 °C), dry (January to April, 49–93 mm) and wet (August to October 122–175 mm) seasons. February is the driest and coldest month (49 mm, −6.0 °C). The sum of degree-days across Kunashir averages ~1700°C, which is the maximum for the Kuril Archipelago (Ivanova 1990).

In addition to the atmospheric circulation patterns, marine currents originating in the North Pacific and Japan Sea influence the Kuril Island climates (Gorbarenko *et al*. 2004, 2014). The warm Soya Current, which enters the southern Okhotsk Sea from the Japan Sea, flows northeastward, paralleling the western coastlines of the southern Kuril Islands (Fig. 1A). The current enters the Pacific Ocean through Bussol' Strait to the north of Urup Island. The Soya and the cooler East Kamchatka currents join on the Pacific side of the Archipelago to form the cool Oyashio Current. This circulation pattern results in warmer conditions in the southern as compared with the northern islands. The north–south-oriented volcanic ridges on the Kuril Islands provide an effective barrier to the cool fogs and winds associated with the Oyashio Current, which is an additional factor causing relative warmth along the western coasts of the southern Archipelago (Razjigaeva *et al*. 2002).

The vegetation of Kunashir Island can be classified into three forest types: (i) cool-temperate broadleaf; (ii) boreal conifer; and (iii) a mix of boreal conifer and cool-temperate broadleaf (Vorobiev 1963; Alekseeva, 1983; Barkalov 2009). The southern part of the island, where

Glukhoye Lake is located, supports both cool-temperate broadleaf forest and mixed conifer–broadleaf forest. Broadleaf taxa include *Quercus crispula*, *Quercus dentata*, *Acer mayrii* and *Acer ukurunduense*, with *Kalopanax septemlobus*, *Ulmus lacintata* and *Ulmus japonica*, while less common, thermophilus species, such as *Magnolia hypoleuca*, *Fraxinus manshurica*, *Betula maximowicziana*, *Alnus japonica* and *Syringa amurensis*, are also present. Conifers in the southern part of the island are *Abies sachalinensis*, *Picea glehnii*, *Picea ajanensis*, *Larix leptolepis* and *Taxus cuspidata*. Boreal conifer forest in northern Kunashir is dominated by *Abies sachalinensis* but also includes the evergreen species found in the southern conifer communities.

The Kunashir vegetation is also characterized by five altitudinal zones, although their geographical distribution varies across the island. These zones include: (i) cool-temperate broadleaf forest (~0–400 m a. s. l. in the south; restricted to river valleys and elevations below 200 m a. s. l. in the north); (ii) boreal conifer forest (~200–700 m a. s. l. in the northern and central island); (iii) *Betula ermanii* forest (~400–600 m a. s. l. in the north); (iv) *Pinus pumila* shrub tundra (typically ~600–800 m a. s. l. but can extend to 1500 m a. s. l. in the southern and central island) – note that *Pinus pumila* also grows in thickets that are scattered in both the conifer and broadleaf forests; and (v) alpine tundra, found at the highest elevations beyond *Pinus pumila* shrub tundra. In addition, coastal forb or forb–graminoid meadows can be extensive, often covering large, stabilized dune fields. Ericales occur as shrubs or subshrubs in all of the vegetation zones as well as in meadows found in moist, lowland areas (~0–200 m a.s.l.) and along marine terraces, coastal cliffs and the flanks of volcanoes. These taxa are also a component of lowland forb–graminoid meadows. The most common ericaceous species include *Empetrum sibiricum*, *Rhododendron aureum*, *Phyllodoce* spp., *Arctica nana* and *Cassiope lycopodioides*. *Sasa kurilensis* is a dominant taxon on lower to mid-elevation slopes (i.e. below 400 m a.s.l.) throughout the island. Additionally, numerous microhabitats, which are related to the influences of marine currents, topography and hot spring activity, can be found on the island (Alekseeva, 1983).

Glukhoye Lake

Glukhoye Lake is located on the Pacific side of southern Kunashir Island (Fig. 1C) on the eastern edge of the Sernovodsky Isthmus. The lowland around the lake is composed of a mix of unconsolidated Quaternary sediments of multiple origins, as described above. A small hill (~40 m a.s.l.) separates Glukhoye Lake from the Sernovodka River, the present-day Peschanoye Lake outlet. The hill itself is part of the Danilov Upland (maximum elevation of ~150 m a.s.l.), which borders the isthmus to the north and west. Glukhoye Lake is elongated along a north–south axis with a maximum length of ~700 m, a maximum width of ~325 m and an elevation of ~2 m a. s. l. A bathymetric survey of Glukhoye indicated two separate basins of ~2.4 m water depth in the south/south-central part of the lake with a shallow shelf of ≤1.5 m water depth to the north (Fig. 1D). The lake has two small streams (~140 and 440 m in length) that drain to the north. They terminate in the boggy terrain that characterizes much of the lowland and are not part of the larger Sernovodka River drainage. Small seasonal streams flow into the lake from the western upland. Lemnaceae and *Nymphaea*, the latter being particularly dense in the northern part of the lake, are the major aquatic plants.

Meadows border much of the Glukhoye basin, with relatively extensive boggy areas in the southern and northeastern ends of the lake. Poaceae spp. dominate these meadows, and wetter areas support *Eriophorum gracile*, *Eriophorum vaginatum*, *Juncus* spp. and a variety of wet-to-mesic forbs (e.g. *Iris*, *Polygonum bistorta*, *Rumex* spp., *Equisetum*, *Comarum palustre*, *Menyanthes trifoliata*, *Symplocarpus renifolius*, *Lilium lancifolium* and *Ranunculus* spp.). Disturbed and/or better drained areas are relatively scarce at lower elevations near the lake, but these micro-habitats support more drought-tolerant forbs (e.g. *Artemisia* and other Asteraceae) and graminoids.

Duschekia maximowiczii, often in association with shrub *Salix*, is abundant on lower hillslopes on both sides of Glukhoye Lake, achieving heights of 2–3 m. *Myrica*, while present along the shore, is not common. *Betula*–broadleaf–conifer forest is found below 200 m a. s. l. on slopes that border the lake to the east and west. The main taxa of the mixed forest include *Quercus crispula*, *Alnus japonica*, *Alnus hirsuta*, *Betula ermanii*, *Sorbus commixta*, *Abies sachalinensis* and *Picea ajanensis*. *Sasa kurilensis* is locally abundant on slopes. *Acer ukurunduense*, *Hydrangea* and *Actinidia* are present but not common. *Pinus pumila* occurs as isolated individuals near the lake, but the conifer is more abundant regionally, often forming dense thickets at higher elevations (>200 m a.s.l.).

Material and methods

In summer 2007, a 562-cm-long sediment core (G-1; Fig. 1D) was recovered from one of two central basins in Glukhoye Lake at a water depth of ~260 cm. A plexiglass tube was used to collect the upper, water-rich sediments and a modified Livingstone piston corer (Wright *et al.* 1984) retrieved the remaining sediments. Core sections were split and photographed. Diatom and palynological samples were taken every 10 cm, and samples for geochemical analyses were taken every 20 cm. Radiocarbon analyses were performed in the laboratories at the Interdisciplinary Science Research Institute N.A. Shilo, Far East Branch, Russian Academy of Sciences, Maga-

dan. The lithology was described through visual inspection.

Standard methods were followed to process 1 cm^3 subsamples for pollen analysis following standard procedures for sediments from arctic and sub-arctic lakes (PALE 1994). Samples from the upper part of the Livingstone core were correlated with the plexiglass core using the decline in *Pinus* subg. Haploxylon pollen at ~30 cm; 0–30 cm samples are from the plexiglass core and the remaining samples were taken from the Livingstone core. The individual arboreal and non-arboreal pollen taxon are shown as a percentage of the sum of all identified and unknown terrestrial pollen grains (ΣP). The percentages of spores and aquatics are calculated using ΣP. Palynomorphs were grouped into three subsum categories: Trees & Shrubs; Herbs (terrestrial and aquatic); and Spores. The percentages for each subsum were based on the sum of ΣP + aquatics + spores. Both pollen and diatom data were converted to percentages and plotted using Tilia and Tilia Graph (http://www.tiliait.com), then divided into zones and subzones using the constrained incremental sum of squares method (CONISS). All pollen sums exceeded 300 identified arboreal and non-arboreal taxa with most samples having sums between 500 and 700 grains. The plant taxonomy follows Czerepanov (1995). *Pinus* s/g Haploxylon pollen represents *Pinus pumila*. The distribution of palaeovegetation types is inferred from the relationships between the modern topography and ecology (Vorobiev 1963; Urusov & Chipizubova, 2000; Pietsch *et al*. 2003; Barkalov 2009).

Preparation of diatom samples followed the standard method described by Gleser et al. (1974). A 2 g sample was boiled in a solution of sodium tripolyphosphate with 30% hydrogen peroxide solution. After decantation in distilled water, 100 mL of distilled water was poured into the resulting precipitate. A 0.06 mL aliquot of this mixed suspension was applied to an 18×18 mm cover slip. Identification of the diatom algae and the calculation of diatom valve concentration in the sediment (numbers of valves per 1 g of dry sediment) were performed with an Axioplan 40 light microscope at a magnification of 1000× using immersion oil. The calculation of diatom valve concentration was based on valves per slide transect following the methods described in Avramenko *et al*. (2015). More than 300 valves were counted in each of the preparations. Diatom classification follows AlgaeBase (http://www.algaebase.org). Ecological characteristics of the taxa are taken from Barinova *et al*. (2006).

Organic matter $\delta^{13}C$, sedimentary $\delta^{15}N$, elemental TOC (total organic carbon) and TN (total nitrogen) samples were acid washed (1 M HCl), rinsed five times in deionized water and freeze dried. The samples were then analysed using an elemental analyser to determine TOC and TN concentrations, coupled with a Finnigan Deltaplus isotope ratio mass spectrometer for $\delta^{13}C$ and $\delta^{15}N$ measurements. All isotope values are reported in per mil units (‰) according to the relationship $\delta X = [(R_{sample}/R_{standard}) - 1] \times 1000‰$, where X is the element of interest and R is the measured isotopic ratio. Carbon isotope measurements are relative to the Vienna Peedee Belemnite standard, and all nitrogen measurements are relative to atmospheric nitrogen. Replicate measurements of internal standards, which were run along with TOC, TN, sedimentary $\delta^{13}C$ and sedimentary $\delta^{15}N$ samples, yielded uncertainty in the isotopic measurements of <0.2‰ and coefficients of variation of <5% of the value for the C and N% data.

Radiocarbon dates were converted to calibrated ages using the IntCal13 calibration curve (Reimer *et al*. 2013) in CALIB 7.1 (Reimer *et al*. 2013; Stuiver *et al*. 2020). An age–depth model was then constructed using BACON ver. 2.3 (Blaauw & Christen, 2011; Blaauw & Heegaard 2012). This program divides the palaeorecord into a specified number of sections, based on user-defined core characteristics, and estimates accumulation rates using Bayesian statistics. All ages in the text are presented as calibrated kiloyears before present (cal. ka BP).

Results

Lithology

The 5.62-m-long core (G1), while variable in its sedimentology, has been divided into three lithological units (Table 1). Unit 1 (564–141 cm) has a complex stratigraphy, but it is mostly dominated by silt, which often is mixed with pebbles, gravel and/or sand. Unit 2 (141–107 cm) is composed of peat that includes gravel and sand. Unit 3 (107–0 cm) caps the peat with a layer of silt; the upper 102 cm are characterized by a water-rich gyttja.

Chronology

A total of 13 radiocarbon samples were analysed from Glukhoye Lake (Table 2). Because the core had few plant macrofossils in Unit 1, which comprises the greatest portion of the core, we took four paired macrofossil–bulk sediment samples to compare the age results. In all cases, the paired samples yielded the same age (115 cm, 325–339 cm) or ages that were within one standard error (470 cm, 545–546 cm). These results indicate that there is minimal offset between sample types. However, the age–depth distribution of the median calibrated ages indicates that the results for 40, 139–141 and 250 cm are probably in error, as they do not follow the generally linear pattern evident in the age–depth (Fig. S1) and BACON plots (Blaauw & Christen, 2011; Fig. 2). Where similar ages of paired macrofossil and bulk samples occurred, bulk sediments were used in the age model so that sample type was consistent with the bulk ages used to constrain the upper part of the core. Note that the ages

Table 1. Sediment description, Glukhoye Lake.

Depth (cm)	Age (cal. ka BP)	Sediment description
Unit 3		
0–100	0–2.34	Watery, organic rich gyttja; large bivalve 27–32 cm and 78–80.5 cm
100–102	2.34–2.39	Organic-rich gyttja with peaty inclusions
102–107	2.39–2.51	Silt
Unit 2		
107–141	2.51–3.31	Peat; 139–141 cm peat includes gravel and sand
Unit 1		
141–170	3.31–3.98	Silt
170–174	3.98–4.04	Silt–sand mix with pieces of gravel
174–193	4.04–4.31	Silt
193–250	4.31–5.16	Silt with scattered sand
250–251	5.16–5.17	Sand
251–253	5.17–5.20	Organic-rich silt
253–379	5.20–6.74	Silt with scattered sand and gravel; sand layer at 254.5–255.3 cm; rock fragment 341.5–343 cm; 369–369.5 gravel layer
379–404	6.74–6.95	Silt with scattered organic material
404–448	6.95–7.46	Silt
448–454	7.46–7.53	Pebble layer
454–466	7.53–7.67	Silt
466–564	7.67–8.17	Silt with scattered small rock fragments

younger than 2590 cal. ka BP (0–115 cm) presented in the text and figures are based on a linear extrapolation of the age model. As the sediment type does not change over this interval, we believe that this is a reasonable approach to provide a provisional age scheme for the latest Holocene. Nonetheless, ages in this part of the core are considered as tentative and should be used with caution. The use of Early (*c*. 11.7 to 8.2 cal. ka BP), Middle (*c*. 8.2 to 4.2 cal. ka BP), and Late (*c*. 4.2 cal. ka BP to present) Holocene follows Walker *et al*. (2019).

Diatoms

The sediments of Glukhoye Lake yielded a rich and diverse diatom flora (Figs 3, 4, Table S1). The core includes 453 taxa that belong to different ecological groups (e.g. marine, brackish-water, freshwater, bog, benthic, tychoplanktonic, planktonic). The changes in valve concentrations and the ratios of representatives of the ecological groups formed the basis for the identification of the four diatom zones (DZ; Table 3). DZ1 is characterized by assemblages with a high species richness of marine and brackish taxa. DZ2 shows some of the highest valve concentrations in the Glukhoye record. It is also characterized by high species richness within the freshwater planktonic and tychoplanktonic diatom categories. DZ3 is marked by a clear decrease in the concentration of diatom valves and the predominance of bog taxa. The species richness of freshwater tychoplanktonic taxa and valve concentrations again increases in DZ4. Variations in diatom percentages within some zones have resulted in the delineation of two subzones in DZ2 and three subzones in DZ1. DZ2.1 is characterized by high percentages of the freshwater tychoplanktonic *Staurosira venter*. DZ2.2 is distinguished by high percentages of the freshwater tychoplanktonic *Staurosira construens* var. *exigua* and the planktonic *Aulacoseira italica*. DZ1.1 and DZ1.3 are marked by high percentages of the marine taxon *Paralia sulcata*.

Geochemistry

Changes in organic carbon content and its $\delta^{13}C$ composition generally follow the major lithological change at ~140 cm (Fig. 5). Organic carbon contents range from ~1 to 29% and are significantly higher in the upper 140 cm. The highest organic content occurs between ~140 and 80 cm. The $\delta^{13}C$ values are relatively high (~−25 to −21‰) below ~200 cm, with maximum values occurring between 200 and 250 cm. Values decline between ~200 and 160 cm, above which they average ~−29‰. The TOC/TN weight ratios range between ~12 and 20. There is no strong trend in the data, but the highest values occur between ~80 and 120 cm. The $\delta^{15}N$ values range between ~1 and 5‰. These values are

Table 2. Radiocarbon and calibrated ages, Glukhoye Lake. Dates not used in the age model are indicated by an asterisk.

Depth (cm)	Material dated	Date (^{14}C a BP)	Median calibrated age (cal. a BP)	2σ calibrated age (cal. a. BP)	CAMS laboratory number
40*	Bulk	5160±30	5920	5890–5990	152311
115	Bulk	2505±30	2590	2490–2735	152312
115	Bulk	2506±30	2590	2490–2735	152313
139–141*	Plant macrofossil	1150±40	1065	970–1175	136956
170	Bulk	3680±35	4020	3900–4090	143084
250*	Bulk	6970±100	7800	7620–7970	152314
325–330	Bulk	5615±30	6390	6310–6450	153935
325–339*	Plant macrofossil	5610±35	6380	6310–6460	153938
393	Plant macrofossil	5950±35	6780	6680–6860	136957
470	Bulk	7120±35	7950	7920–8010	153936
470*	Plant macrofossil	7165±35	7980	7930–8030	153939
545–546	Bulk	7145±35	7970	7930–8020	153937
545–546*	Plant macrofossil	7085±35	7915	7840–7970	153940

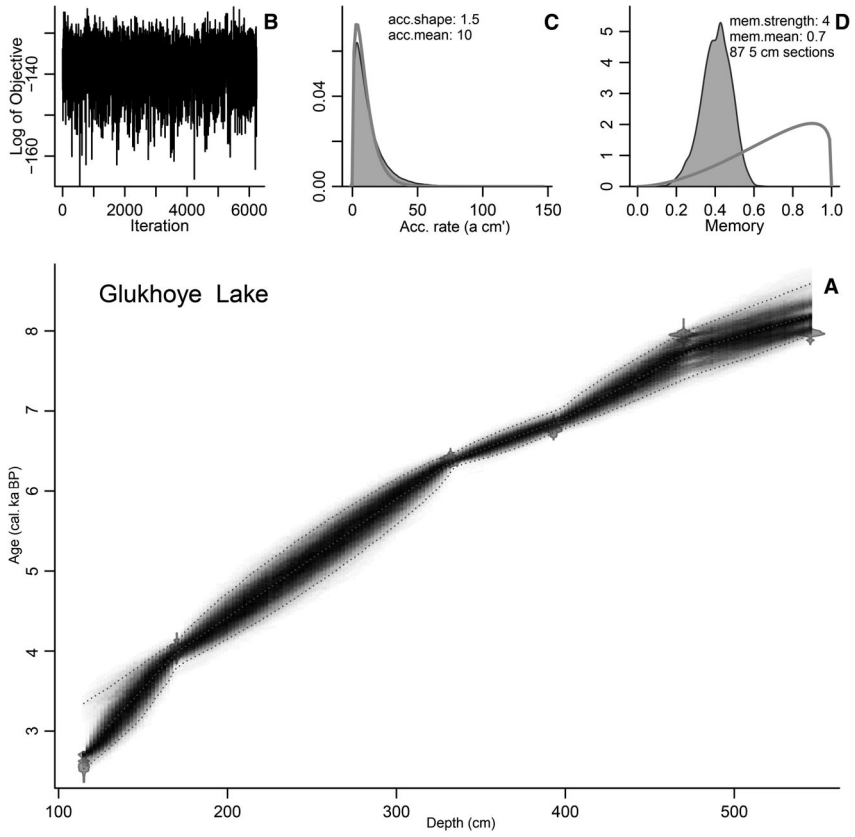

Fig. 2. Age model for Glukhoye (G-1) using Bacon age-modelling software (Blaauw & Christen, 2011). Bacon Manual – v. 2.2. http://www.chron.qub.ac.uk/blaauw/bacon.html. The bottom panel shows the calibrated ages and the age–depth model. The black curve indicates the optimal model based on weighted mean ages, whereas the grey stippled portion reflects 95% confidence intervals. The upper panels indicate the following: left = history of Markov Chain Monte Carlo iterations; middle = distributions for the accumulation rate illustrating prior (grey line) and posterior (grey infilled curve) distributions; right = distributions for memory illustrating prior (grey line) and posterior (grey infilled curve) distributions.

relatively low in Unit 3 (~2‰) but are higher (> ~4‰) between 220 and 330 cm.

Palynology

Six pollen zones (PZ) were defined for the Glukhoye record (Fig. 6). Zone boundaries do not correspond to changing depositional environments, as indicated by the diatom data (Table 3). Thus, the variations in the palynological record reflect changes in the palaeovegetation. Tree and shrub pollen dominate in zones PZ2–PZ6, and the percentages of total herb taxa vary between 20 and 40% of total pollen and spores below ~230 cm and from 40 to 50% in samples from 230 to 0 cm. The total percentages of spores decline in PZ4–PZ6, caused mostly by the decrease in Polypodiaceae. PZ1–PZ3 are characterized by broadleaf deciduous species with *Quercus* being the most dominant taxon. The role of *Quercus* is less in assemblages of the upper three zones, but *Betula* becomes an important component of these spectra. Conifer taxa are more common in PZ4–PZ6, although *Pinus* s/g Haploxylon shows modest values in PZ1. The rise in conifer pollen is gradual in PZ4 with the *Picea* sect. Eupicea and *Abies* pollen reach maximum percentages in PZ5. Both taxa decline sharply in PZ6, where *Pinus* s/g Haploxylon shows a second percentage peak. *Larix* occurs in trace amounts in the upper three zones. Pollen from more temperate flora, such as *Tilia*, *Fagus*, *Sorbus*, *Acer*, *Magnolia* and *Fraxinus*, occur sporadically and in trace amounts throughout the record. *Ulmus* pollen is found in all zones but generally is <5%; *Juglans* pollen occurs consistently in PZ1–PZ4 with maximum values (~5 to 7%) in PZ2 and PZ3. Graminoids dominate the herb taxa; maximum Poaceae percentages (~15–30%) occur in the lower two zones. Saxifragaceae, Polygonaceae, Primulaceae, Lamiaceae and *Iris* have the highest percentages within the minor taxa group, but they do not exceed 5%. Aquatic pollen is restricted to sporadic occurrences as trace amounts in PZ3–PZ6, with Nymphaceae being the most common taxon. Polypodiaceae spores are abundant in PZ1–PZ3 (up to 50%) but are reduced to ~5% in the remaining zones. Osmundaceae is also highest in the lower zones, but the spores are generally <10% with decreasing values up-core. *Sphagnum* occurs consistently in all zones but is <10%.

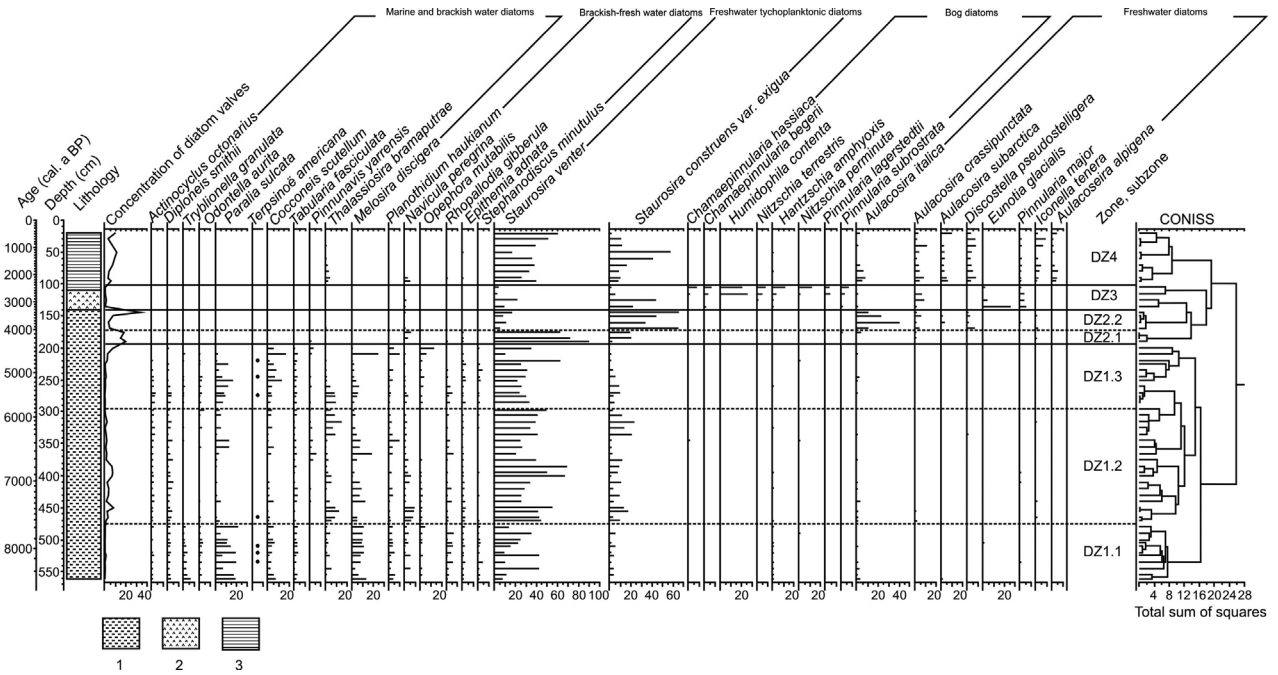

Fig. 3. Percentages of major diatom taxa arranged in ecological groups. Lithological units are: 1 = organic-rich silt; 2 = peat; 3 = silt and mix of silt and sand. See Table 1 for more details. Note that the ages younger than 2590 cal. ka BP (0–115 cm) are based on a linear extrapolation of the age model and should be considered as tentative.

Discussion

In this section, we will first describe the varying depositional environments represented in the Glukhoye core and the probable origin of the basin. We next will consider Middle to Late Holocene vegetation as inferred from the Glukhoye data and compare these results with the palaeovegetation as interpreted from the sections for the Greater Kuril Ridge. Finally, we will re-examine the palaeoclimate model proposed by Korotky *et al*. (1996, 2000) in light of the data provided by the lacustrine records in the Kuril Islands.

Depositional environments of the Glukhoye basin

The DZ1 diatom assemblage indicates that the Glukhoye basin was a brackish lagoon *c*. 8.2 to 4.3 cal. ka BP, as shown by the moderate to high percentages of *Actinocyclus octonarius*, *Cocconeis scutellum*, *Melosira discigera*, *Paralia sulcata*, *Thalassiosira bramaputrae* and *Tryblionella granulata* (Fig. 3). Korotky *et al*. (1996, 2000) concluded that sea levels in the southern Kurils began to rise *c*. 8.9 cal. ka BP, with a high stand of +2.5–3.0 m p.s.l. (present sea level) between *c*. 7.4 and 6.8 cal. ka BP, a pattern consistent with the encroachment of saline waters into the low-lying Glukhoye basin. However, the presence of brackish and freshwater diatoms indicates that the Glukhoye basin was not dominated by saline water, as would be the case if the entire Sernovodsky Isthmus was flooded by rising sea levels, as proposed by Korotky *et al*. (1996, 2000). The rare occurrence in DZ1 of neritic diatoms, which inhabit depths of >50 m, suggests the existence of a submerged or possibly partially exposed spit, which would inhibit the penetration of marine diatom taxa into the lagoon. A marine transgression of several metres would affect local coastal processes, and in southern Kunashir Island the rise in sea level probably caused a redistribution of eroded coastal sediments and/or of sediments carried to the ocean by the Sernovodka drainage (Korotky *et al*. 1996, 2000). Under such conditions, the build-up of a spit, which restricted the inflow of marine waters to the Glukhoye basin, might be expected.

DZ1 has been divided into three subzones, suggesting some variations in the lagoon environment during the Middle Holocene. The first notable feature of this assemblage is the trace appearance of *Terpsinoë americana* in the earlier and later parts of the zone. This warm-water tropical species is not found today in the coastal waters off Kunashir Island. It is considered a tropical epiphyte that lives in salty and brackish waters to the south of 45°N (Alhonen *et al*. 1984). Its appearance in the Glukhoye record is evidence for warmer sea temperatures between *c*. 8.0 and 7.7 cal. ka BP and between *c*. 5.7 and 4.5 cal. ka BP. These intervals correspond to times of maximum summer temperatures as inferred from the pollen data. Moreover, geochemical and diatom analyses of marine cores from the southern Okhotsk Sea and the northwestern Pacific Ocean indicate that sea surface temperatures were warmer than present from *c*. 8.0 to

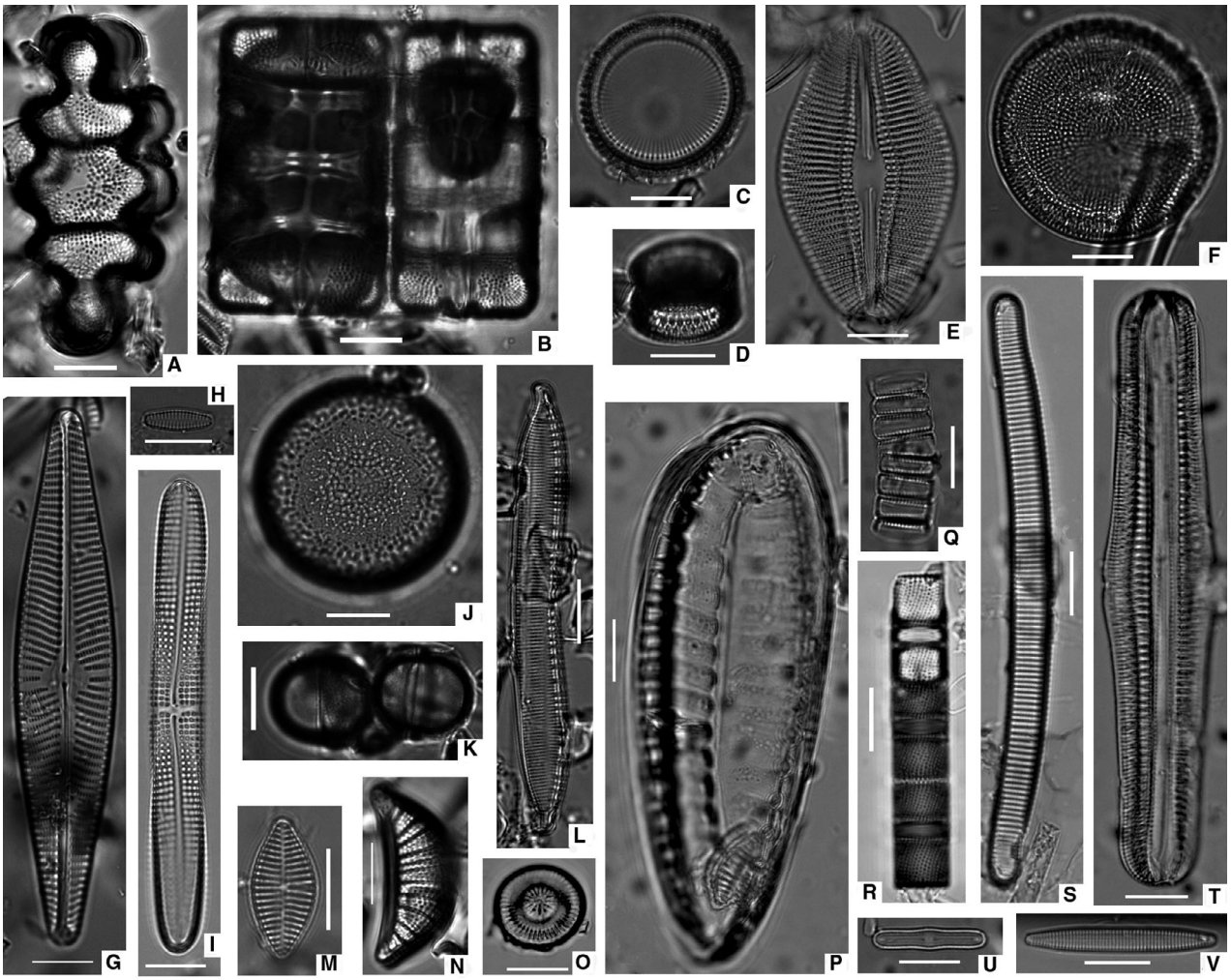

Fig. 4. Photographs of dominant and characteristic diatom taxa, Glukhoye Lake. A, B. *Terpsinoë americana* (A = valve view, B = girdle view). C, D. *Paralia sulcata* (C = valve view, D = girdle view). E. *Diploneis smithii*. F. *Thalassiosira bramaputrae*. G. *Navicula peregrina*. H, Q. *Staurosira venter* (H = valve view, Q = colony part, girdle view). I. *Achnanthes brevipes* var. *intermedia*. J, K. *Melosira nummuloides*. L. *Hantzschia amphyoxis*. M. *Planothidium hauckianum*. N. *Rhopalodia gibberula*. O. *Discostella pseudostelligera*. P. *Iconella tenera*. R. *Aulacoseira italica*. S. *Eunotia glacialis*. T. *Epithemia gibba*. U. *Humidophila contenta*. V. *Staurosira construens* var. *exigua*. The white scale bar indicates a length of 10 μm.

4.5 cal. ka BP (Harada *et al*. 2004, 2014; Okazakia *et al*. 2005; Inagaki *et al*. 2009). The fact that *Terpsinoë americana* occurs sporadically and in only trace amounts in DZ1 suggests that this species was not abundant in the waters off Kunashir Island and that the increase in sea surface temperatures was more modest as compared with other nearby regions (e.g. *Terpsinoë americana* in marine cores off eastern Honshu Island registers up to 60%; Sato *et al*. 1983).

The second feature common to all the subzones is the importance of the freshwater tychoplanktonic diatoms *Staurosira venter* and *Staurosira construens* var. *exigua*. These taxa often occur in sediments as colonies, formed by two to 10 valves (Fig. 4), which may indicate their allochthonous nature in the Glukhoye record. They possibly were transported to the lagoon by freshwater inflow, which today is limited to short, ephemeral streams. If the 30 cm sample can be taken as an approximation of a diatom assemblage associated with the 'modern' drainage pattern, percentages of *Staurosira venter* and *Staurosira construens* var. *exigua* in DZ1 are generally lower or are similar to the modern value. This comparison suggests that if the species were transported to the lagoon via streams, then it is probable that the Middle Holocene inflow to the basin was like that seen today. This similarity further suggests that there was no significant alteration of the drainage patterns in this part of the Sernovodsky Isthmus. However, the formation of lagoons and embayments associated with a proposed marine transgression (Korotky *et al*. 1996, 2000) logically would result in some changes to the drainage patterns within the Isthmus. The pollen data do not indicate an

increase in annual or seasonal precipitation (see the section below on the vegetation history). Thus, if the ancient drainage systems were altered, they were related to shifts in stream gradients and perhaps sediment load caused by rising sea levels, rather than by increased runoff associated with changes in precipitation. Because other freshwater taxa are few and are represented by single valves, it is possible that currents carried *Staurosira venter* and *Staurosira construens* var. *exigua* to the coring site from more desalinated parts of the lagoon.

Table 3. Comparison of ages and depths of pollen and diatom zones.

Pollen zones (PZ)	PZ Age, cal. a BP (depth, cm)	DZ Age cal. a BP (depth, cm)	Diatom zones and subzones (DZ)
PZ6	0–1125 (0–48)	0–2400 (0–102)	DZ4
PZ5	1125–2250 (48–96)	2400–3275 (102–140)	DZ3
PZ4	2250–4050 (96–175)	3275–4340 (140–195)	DZ2
		3275–4010 (140–172)	DZ2.2
		4010–4340 (172–195)	DZ2.1
PZ3	4050–6470 (175–345)	4340–8170 (195–562)	DZ1
		4340–5820 (195–295)	DZ1.3
		5820–7770 (295–475)	DZ1.2
		7770–8170 (475–562)	DZ1.1
PZ2	6470–7940 (345–505)		
PZ1	7940–8170 (505–545)		

The third common feature in DZ1 is the low total concentrations of diatom valves (TCD), excepting a modest increase in the lower part of DZ1.2. Low diatom concentrations can indicate a high-energy hydrological setting, which is reasonable given the deposition of coarse sediments in the lagoon (Unit 1; Table 1). The low percentages of TOC and $\delta^{13}C$ throughout DZ1 also are consistent with a high-energy environment under the influence of marine carbon sources (e.g. more wave action within the basin would result in less deposition of material of low density and small size). The decrease in the planktonic sublittoral species *Paralia sulcata* and a slight increase in sublittoral benthic diatoms (e.g. *Cocconeis scutellum*, *Opephora mutabilis*, *Planothidium hauckianum*), particularly in the lower part of DZ1.2, indicate a slight decline in water levels in the lagoon *c*. 7.8 to 6.8 cal ka. BP. A parallel increase in %TOC in lower DZ1.2 also suggests the occurrence of a lower-energy depositional environment as compared with other parts of DZ1.

The cause of the lowered water levels is somewhat puzzling. The decline in the percentages of *Paralia sulcata*, the absence of *Terpsinoë americana* and a slight increase in the abundance and diversity of freshwater allochthonous diatoms in lower DZ1.2 may reflect greater river runoff into the Glukhoye basin. However, the palynological data do not indicate an increase in precipitation, suggesting that the shift in the diatom complex is most likely related to a change in drainage within the Glukhoye catchment. Korotky *et al*. (1996, 2000) noted a slight marine regression *c*. 6.5 to 6.2 cal. ka BP. Although the timing is not exactly that of lower DZ1.2, perhaps a coastline reconfiguration or shift in coastal sediment load (e.g. from coastal inflow of redeposited sediments from the Sernovodka drainage and/or the influx of coastal shelf sediments) as related to a modest change in sea level may have contributed to the build-up of the barrier bar and the consequent lowered water levels within the lagoon.

Like DZ1.1, DZ1.3 (*c*. 5.8 to 4.3 cal. ka BP) is characterized by low concentrations of diatom valves, an increase in percentages of the sublittoral, brackish-marine species *Paralia sulcata*, and a more consistent appearance of *Terpsinoë americana*. The frequency of taxa (e.g. *Cocconeis scutellum*, *Opephora mutabilis*, *Planothidium hauckianum*) that grow on macroalgae also increases. These data indicate a decreasing water level in the Glukhoye basin. The sea level history proposed by Korotky *et al*. (2000) indicates a regression to modern levels or slightly below modern between *c*. 5.7 and 4.5 cal. ka BP. This reconstruction seems inconsistent with the Glukhoye data, which indicate the persistence of a brackish lagoon, albeit one that was perhaps slightly shallower than previously.

DZ2 (*c*. 4.3 to 3.3 cal. ka BP) marks the transformation of the brackish lagoon into a freshwater basin. DZ2.1 (*c*. 4.3 to 4.0 cal. ka BP) is characterized by the highest frequency of *Staurosira venter*, indicating the increased importance of freshwater flow to the basin. Marine (e.g. *Pinnunavis yarrensis*, *Paralia sulcata*, and *Diploneis smithii*) and brackish (e.g. *Rhopalodia gibberula*, *Navicula peregrina*) taxa are present in low frequencies in DZ2.1, indicating the continued but minor influx of saline water to the basin (e.g. during highest tides). DZ2.2 (*c*. 4.0 to 3.3 cal. ka BP) is distinguished by the dominance of the freshwater planktonic diatom *Aualcoseira italica*. The presence of *Aualcoseira* suggests an increase in eutrophicity (Donar *et al*. 1996; Gibson *et al*. 2003; Juracek, 2003; Kirilova *et al*. 2010). By this time, the Glukhoye basin no longer had any connection to Pacific waters. The occurrence of *Aualcoseira*, the richness of the diatom taxa and the presence of the large-valved *Iconella* taxa indicate a continued warming of the basin's waters. The palynological data suggest that the onset of lake formation corresponds to a climate that, while still warmer than present, was beginning to cool, as

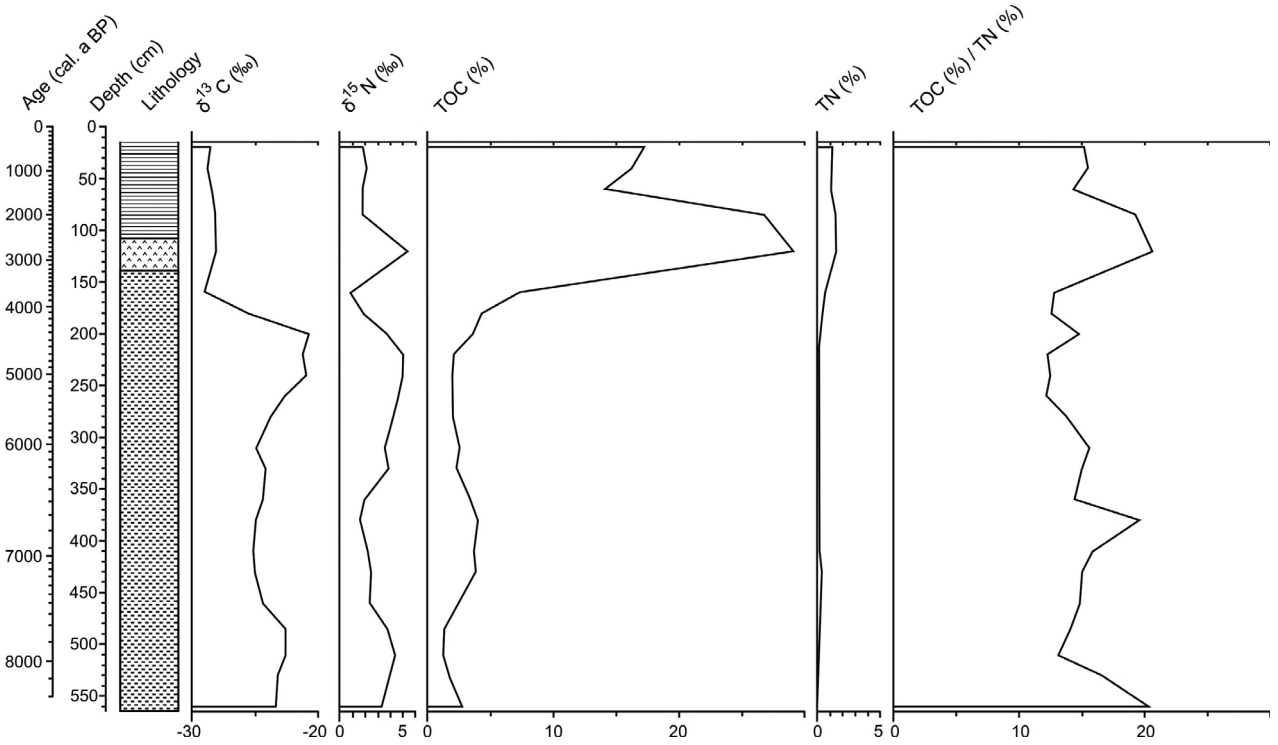

Fig. 5. Geochemical data, Glukhoye Lake showing organic matter (δ^{13}C), sedimentary nitrogen (δ^{18}N); carbon (C%) and nitrogen (N%) weights and weight ratios (C%/N%). δ^{13}C and δ^{18}N are expressed as parts per mil (‰). C, N and C/N are shown as weight percentages. See Fig. 3 for the key to the lithology. Note that the ages younger than 2590 cal. ka BP (0–115 cm) are based on a linear extrapolation of the age model and should be considered as tentative.

indicated by the introduction of conifer trees into the forest.

According to Korotky *et al*. (2000), the DZ2 interval encompasses sea levels that were both slightly lower and slightly higher than present (+1.2 to 1.5 m p.s.l.), the latter occurring *c*. 4.5 to 3.6 ka cal. BP. Rising sea levels are inconsistent with a shift from a brackish lagoon to a freshwater lake, presuming that the marine waters simply flooded the present-day lowlands surrounding the Glukhoye basin. If the age models are accurate for both the lake core and the sections, then the Glukhoye data suggest that coastal processes (e.g. accumulation of a larger and/or higher barrier bar to block marine incursion, blockage of the lagoon inlet with the formation and/or shifts in coastal dune localities) were the main influences in changing the depositional environments in the Glukhoye basin during DZ2.

The organic geochemistry associated with DZ2 reflects an increase in the preservation of organic matter and a greater influence of the terrestrial carbon cycle on the organic material beginning *c*. 4.1 cal. ka BP, as the basin changed from a lagoon to a lake. These data suggest the presence of a setting that: (i) was more protected from wave activity, thereby limiting the removal of fine-grained materials; and (ii) had a greater freshwater influence. These interpretations are consistent with those based on the diatoms and the core lithology, which show the Late Holocene establishment of a freshwater lake in the Glukhoye basin.

The diatom complex in the lower part of DZ3 (*c*. 3.3 to 2.4 cal. ka BP) reflects the transition from a lake to a bog as indicated by *Aulacoseira crassipunctata*, *Eunotia glacialis*, *Pinnularia major* and *S. construens* var. *exigua*. The upper part of the zone with *Chamaepinnularia hassiaca*, *Chamaepinnularia begeri*, *Nitzshia perminuta* and *Pinnularia subrostrata* marks the establishment of a bog ecosystem, with the presence of *Humidophila contenta*, *Nitzschia terrestris* and *Hantzschia amphyoxis* indicating the occurrence of soil-forming processes. A reduction in Polypodiaceae spores and the appearance of trace amounts of Nymphaceae and *Sparganium* pollen in PZ4 and PZ5 (Fig. 6) also suggest a shallowing of the freshwater basin with an expansion of boggy environments near the lake. The higher organic content *c*. 3.3 to 2.6 cal. ka BP shown by the high C/N percentages is consistent with the presence of peaty sediments in the Glukhoye core. Additionally, δ^{13}C values are in accord with a non-marine setting.

The establishment of boggy terrain may indicate a shift in larger-scale climatic forcings that caused a decrease in precipitation, which in turn resulted in a decline in river and/or overland flow into the lake. The shift in hydrology would lead to the lake's desiccation, and ultimately the formation of a bog in the Glukhoye basin. The moderate

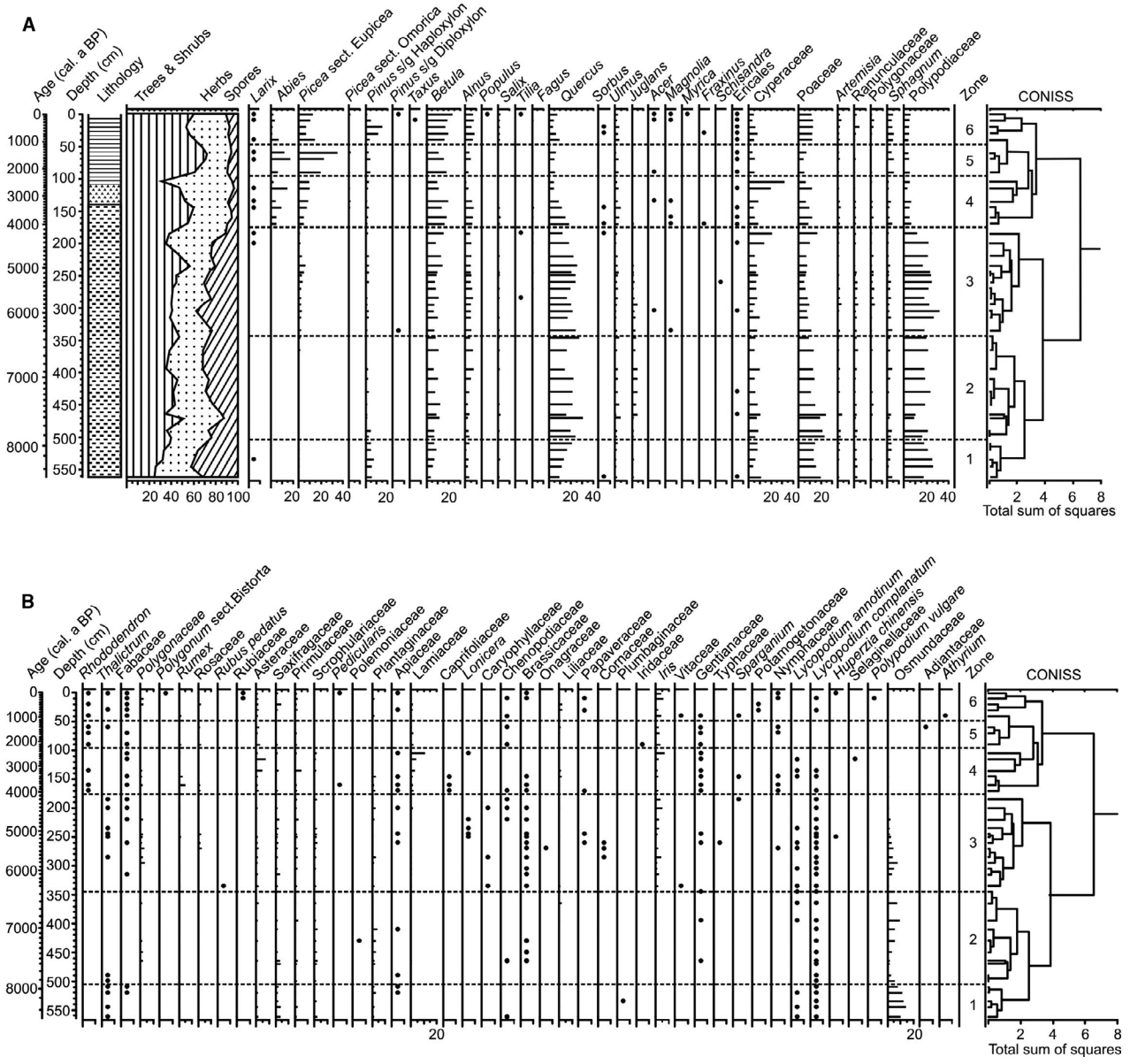

Fig. 6. Percentages of major (A) and minor (B) pollen and spore taxa, Glukhoye Lake. Dark circles indicate taxa that are <2%. See Fig. 3 for the key to the lithology. Note that the ages younger than 2590 cal. ka BP (0–115 cm) are based on a linear extrapolation of the age model and should be considered as tentative.

increases in *Picea* and *Abies* pollen, if representing *Picea glehnii* and *Abies sachalinensis*, are consistent with the presence of cold, wet soils associated with boggy terrain. The occurrence of cool fogs would also favour these conifers and indirectly provide additional moisture to the local landscape. The diatom data suggest that soils ultimately formed on the bog's surface as moisture input decreased and/or substrates became better drained. Here again the palynological record does not indicate any significant decline in effective moisture, although conditions were cooling. Thus, the changes from a lake to a bog to a soil, while reflecting a regional shift to cooler and perhaps slightly wetter climates, appear most likely to have been the result of local changes related to overland or groundwater flow.

DZ4 (*c*. 2.4 cal. ka BP to present), as indicated by *Staurosira venter*, *S. construens* var. *exigua*, *Aulacoseira crassipunctata*, *Aulacoseira subarctica* and *Discostella pseudostelligera*, indicates a second interval of freshwater dominance and the establishment of the present-day Glukhoye Lake. Depleted values of $\delta^{13}C$ in the core's organic remains are consistent with freshwater sources of carbon being used by the aquatic plants. The palynological data suggest the presence of cooler and moister summer climates between *c*. 2.3 and 1.1 cal. ka BP (note: here and in other parts of the Discussion ages that are

younger than *c*. 2.6 cal. ka BP should be considered tentative as they are based on a linear extrapolation from the last radiocarbon date at 115 cm to the core top). The increase in summer precipitation perhaps led to the flooding of the Glukhoye basin and the formation of a freshwater lake. If lake formation is linked directly to climate, then seasonal water source perhaps shifts from primarily a spring (*c*. 2.4 to 1.1 cal. ka BP) to a winter (*c*. 1.1 cal. ka BP to present) runoff, reflecting the inferred change to an increased snow cover during the latest Holocene as indicated by the pollen data. The appearance of *Iconella tenera* in DZ4 indicates warm waters within the basin over the past *c*. 2.4 cal. ka BP. Although there was moderate climate cooling over the past *c*. 1.1 cal. ka BP, the continued presence of this species suggests that this cooling did not affect the temperature of the lake water. A slight decline in percentages of TOC % and TOC%/TN% could indicate a modest deepening of the lake between *c*. 1.9 and 1.4 cal. ka BP.

Genesis of the Glukhoye basin

Based on preliminary work, Anderson *et al*. (2009) proposed three alternative hypotheses for the genesis of the Glukhoye basin: (i) Glukhoye was once part of a larger Peschanoye Lake, which covered most of Sernovodsky Isthmus (Fig. 1C); (ii) Glukhoye and Peschanoye lakes are both remnants from a time when sea level was higher than present and the isthmus was flooded by marine waters; or (iii) the elongated Glukhoye basin is an abandoned river channel that once drained an older Peschanoye Lake. As described below, a history of the Middle to Late Holocene geomorphology of Kunashir Island (Korotky *et al*. 1996; Razjigaeva *et al*. 2011a, b) describes changes in the timing and types of landforms that are both consistent and inconsistent with the Glukhoye record.

The section-based data indicate that sea levels began to rise starting *c*. 8.9 cal. ka BP, reaching a high stand of *c*. +2.5–3.0 m p.s.l. The final flooding of the land bridge which connected Kunashir Island to northern Japan occurred *c*. 6.9 cal. ka BP (Sato *et al*. 1998; Korotky *et al*. 2005). This marine transgression resulted in the eventual formation of large open bays and lagoons on the Pacific and Okhotsk sides of Kunashir Island, respectively. The flooding of Sernovodsky Isthmus is believed to have occurred at this time. In other areas of the island, the erosion of coastlines related to the transgression resulted in the build-up of barrier bars and numerous coastal lakes. Eventually, storm ridges developed, causing the demise of most of the lakes. A minor regression, indicated by the formation of large dunes (up to 20 m high), occurred *c*. 5.4 cal. ka BP. At this time, the marine strait was still present in the area of the modern Sernovodsky Isthmus, but it was divided by narrow 'land bridges'. Two additional transgressions, from *c*. 4.5 to 3.6 and from *c*. 3.1 to 2.8 cal. ka BP, are marked by the erosion of coastal dunes and the formation of large sandy beaches and small estuarine lagoons. Two intervals of sea level lowering led to coastal dune formation and infilling of lagoons, the latter resulting in the closure of the coastal bays on each end of Sernovodsky Isthmus at *c*. 2.3 to 1.5 cal. ka BP. This period is also characterized by the subsequent development of freshwater lakes on the island.

The palaeodata preserved in the Glukhoye core indicate a simpler environmental history (i.e. a brackish lagoon, followed by a freshwater lake, a bog, and again a freshwater lake; Fig. 7) as compared with that reconstructed from the Kunashir sections. Nonetheless, the Glukhoye data are consistent with the proposed pattern of marine incursion and subsequent formation of coastal lakes and peats. The lithological and diatom data from the sections indicate the development of lagoons and then freshwater lakes between *c*. 4.5 and 1.5 cal. ka BP, whereas the Glukhoye data suggest that a lagoon phase ended by *c*. 4.3 cal. ka BP. Such differences in timing are to be expected given the piecemeal nature of the palaeoenvironmental record preserved in the sections and the relatively few radiocarbon dates and the limited spatial distribution of both lacustrine and section sites. Nonetheless, there are clear parallels in both data types that can be used in evaluating the genesis of the modern Glukhoye Lake.

Revisiting the first of the three hypotheses about the history of the Glukhoye basin, the low-lying topography of the Isthmus would not limit the size of Peschanoye Lake, and modern elevations are similar (~2.0 m a.s.l.) between Peschanoye and Glukhoye lakes. Tectonic activity may have altered the relative elevations over time, but there is no evidence to suggest that the area was not a lowland throughout the Middle to Lake Holocene (Korotky *et al*. 1996; Razjigaeva *et al*. 2017). However, large shifts in precipitation and increased river inflow to the Isthmus would be needed to connect both freshwater lakes. The palynological data from Glukhoye and from the Kunashir sections (Razjigaeva *et al*. 2011a, 2013) do not support such a large increase in either rain or snow fall.

Turning to the second hypothesis, the Glukhoye diatom record indicates that the basin initially was filled with brackish water, reflecting some inflow from the Pacific. The occurrence of a lagoon between *c*. 8.2 and 4.3 cal. ka BP might support the idea that the Isthmus was once flooded, forming a strait between the Pacific Ocean and the Okhotsk Sea. The formation of exposed areas cross-cutting the isthmus *c*. 5.4 cal. ka BP possibly represents the initial separation of the Peschanoye and Glukhoye basins. However, if a true marine strait were established during the Middle Holocene, the Glukhoye diatoms should reflect greater salinity and would include taxa associated with a greater marine influence (e.g. an open bay as opposed to a brackish lagoon, the latter probably formed by a barrier bar). Unfortunately, we do

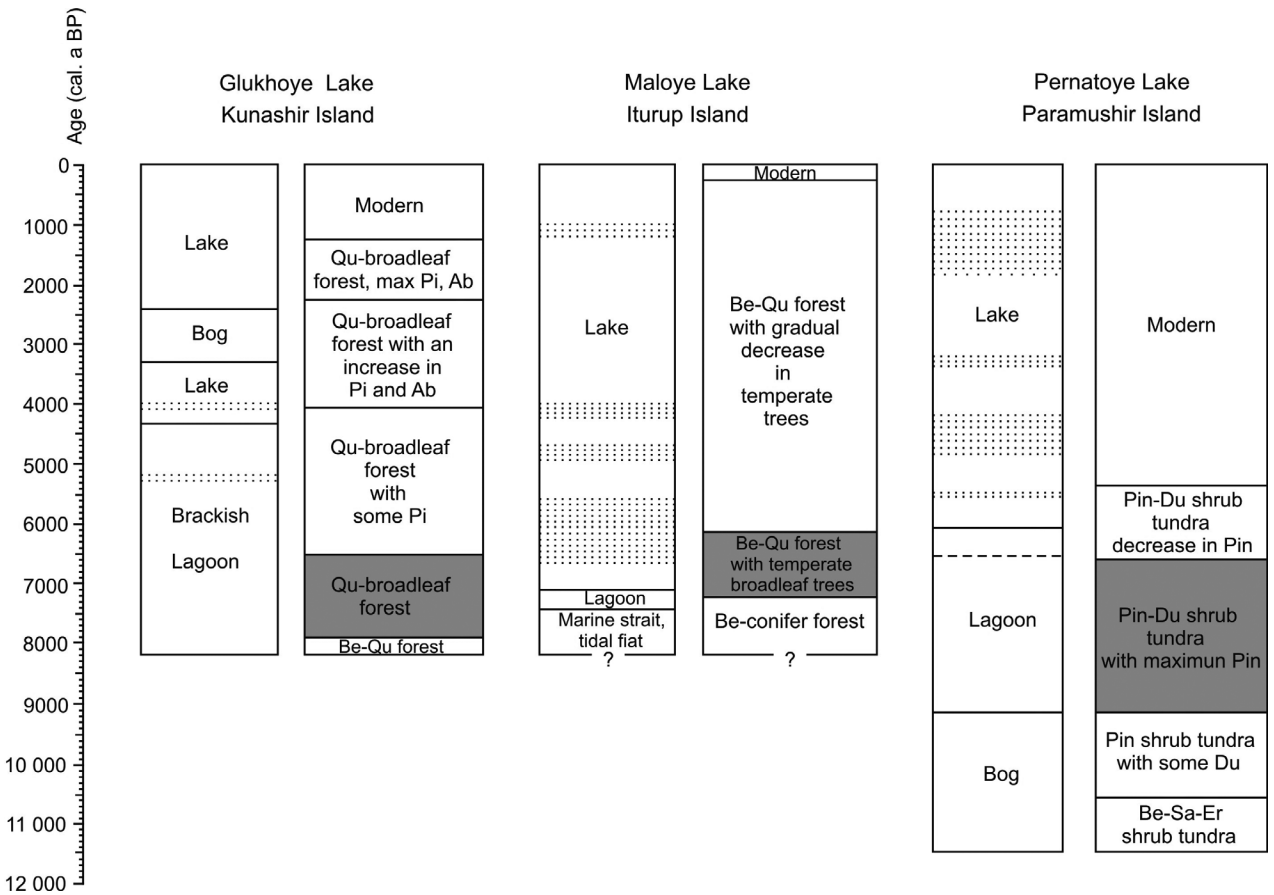

Fig. 7. Schematic diagram showing Holocene changes in depositional environments and vegetation histories from Glukhoye Lake, Maloye Lake (Iturup Island; Lozhkin *et al.* 2017) and Pernatoye Lake (Paramushir Island; Lozhkin *et al.* 2010; Anderson *et al.* 2015). See Fig. 1 for the location of the islands. The key to the abbreviations in the palaeovegetation column is: Ab = *Abies*; BE = *Betula*; Du = *Duschekia*; Er = ericads; Pi = *Picea*; Pin = *Pinus pumila*; Qu = *Quercus*; Sa = *Salix*. Question marks at the base of the Maloye columns indicate an uncertain basal age. Dotted areas in the basin history delineate sand layers. The dashed line in the Pernatoye basin history marks the shift from a saline to brackish lagoon. Grey shading in the columns indicates the palaeovegetation associated with the Holocene thermal optimum.

not have a core from the larger lake (whose maximum depth is 36 m) nor any material from exposures near the lake. Thus, we cannot establish whether marine waters once filled the Peschanoye basin. However, the Glukhoye data do not support the establishment of a marine strait nor the presence of a large open bay, at least on the Pacific side of Kunashir Island.

The third hypothesis suggested that the Glukhoye basin was once part of the Peschanoye drainage. The current Peschanoye outlet flows to the north of Glukhoye Lake. Glukhoye Lake and the Peschanoye outlet are separated by boggy terrain and a small hill (~40 m a.s.l.). Given the modern topography, the outlet could once have included Glukhoye Lake. However, we lack evidence of alluvial terraces that would suggest an ancient river that once flowed through the Glukhoye basin to the Pacific and then was subsequently abandoned. Although diatoms indicate a period when the basin supported a boggy landscape, thus suggesting changes to the local hydrology (e.g. drainage pattern, groundwater), there is no evidence in the diatom complex nor the sedimentology of the Glukhoye core that the basin was part of a riverine system. Rather it seems that the history of the Glukhoye basin mainly records the interactions of coastal dynamics and local changes in hydrology rather than being formed by any of the processes we originally considered in our hypotheses.

The Middle and Late Holocene vegetation of southern Kunashir Island

The earliest vegetation represented in the Glukhoye record was *Betula–Quercus* forest with an understory of *Alnus* and *Pinus pumila* shrubs (PZ1; *c.* 8.2 to 8.0 cal. ka BP; Fig. 6). Other broadleaf trees, such as *Ulmus*, *Juglans* and *Fagus*, were present but not common. *Pinus pumila* also grew at higher elevations. Graminoid species were an important element on the landscape, most likely associated with lowland meadows. Although its pollen is not distinguishable from that of other Poaceae, *Sasa* was probably present by the early Middle Holocene. Today *Sasa kurilensis* forms dense thickets in open areas of the

forest. Like *Pinus pumila*, it requires sufficient snow cover to protect its leaves from frost damage (Suslov 1961; Andreev 1980). The occurrence of *Sasa* is supported indirectly by the establishment of *Pinus pumila*, implying sufficient snow cover, and by Polypodiaceae, which indicates openings in the forest canopy. The presence of *Sphagnum* and Polypodiaceae suggests the occurrence of mesic to boggy substrates and forested habitats near the lake. Temperatures were more moderate than present, with the steady increase in *Quercus* pollen in PZ1 suggesting a gradual warming between *c*. 8.2 and 8.0 cal. ka BP. Section data from southern Kunashir Island indicates the establishment of a similar vegetation to that inferred from the Glukhoye record. However, the sections indicate that *Betula–Quercus* forest persisted until *c*. 7.5 cal. ka BP and that climates were warmer than modern during the Early to Middle Holocene transition (Razjigaeva *et al*. 2013).

Between *c*. 8.0 and 6.5 cal. ka BP (PZ2), broadleaf forest became more widespread in the vicinity of Glukhoye Lake. These communities were dominated by *Quercus* but also included *Juglans*, *Ulmus*, tree *Betula* and tree *Alnus*. The reduction in *Pinus* s/g Haploxylon pollen indicates the disappearance or rare occurrence of *Pinus pumila* in the region. Meadows probably persisted in wet low-lying areas but may not have been as prevalent as previously (e.g. slight reductions in *Sphagnum* spores and Poaceae pollen). Polypodiaceae continued to be an important element in the forest groundcover. The increase in more temperate tree taxa (e.g. *Juglans* and to a lesser extent *Ulmus*; consistently high percentages of *Quercus*) indicates a continuation in the trend towards increased warmth noted for zone PZ1. However, zone PZ2 reflects the warmest climate in the Glukhoye record. The decline in *Pinus pumila* suggests drier conditions during the cold season (Andreev 1980; Kozhevnikov 1981). During this interval, section data indicate that a cool-temperate *Quercus*–broadleaf forest spread throughout Kunashir Island, extending northward to Iturup Island and southward into the Lesser Kuriles (Korotky *et al*. 1996, 2000; Razjigaeva *et al*. 2002, 2004, 2011a; Lyaschevskaya & Ganzei 2011; Lozhkin *et al*. 2017). In contrast to the Glukhoye record, Korotky *et al*. (1996, 2000) concluded that the entire Archipelago experienced maximum Holocene warmth between *c*. 7.5 and 5.7 cal. ka BP.

While the *c*. 8.0 to 6.5 cal. ka BP interval marks the warmest part of the Glukhoye record, warmer than modern conditions continued in PZ3 (*c*. 6.5 to 4.1 cal. ka BP). *Quercus*, *Juglans* and *Ulmus* were common elements of the broadleaf forests, which also included *Fagus*, *Tilia*, *Acer*, *Magnolia* and *Shizandra*. Low percentages of *Picea* sect. Eupicea pollen, representing *Picea ajanensis* and/or *Picea glehnii*, suggest expansion of the conifers into the region. The modest presence of the conifers indicates a decline in summer temperatures as compared with the previous zone. Korotky *et al*. (2000) suggested that a weak cooling, associated with a slight marine regression, occurred at *c*. 6.5 to 6.2 cal. ka BP on Kunashir Island. The lake records from both Kunashir and nearby Iturup islands (Lozhkin *et al*. 2017) do not indicate such a brief climatic reversal.

Quercus–broadleaf forests persisted in the lowlands and along the coast *c*. 4.1 to 2.3 cal. ka BP (PZ4). The modest increase in *Abies* and *Picea* pollen indicates an expansion of conifer forest on hill and mountain slopes and provides additional evidence for the continued cooling trend initially noted for zone PZ3. The moderate but consistent increase in *Betula* pollen as compared with PZ3 reflects its greater role in the vegetation. During this interval, the Glukhoye record is in good agreement with the sections.

Palynological spectra of PZ5 (*c*. 2.3 to 1.1 cal. ka BP) differ from the assemblages in the earlier zones by the maxima in *Abies* and *Picea* pollen, consistent but trace percentages of *Larix* pollen and the final reduction in pollen from broadleaf taxa. This zone marks the increase in dark coniferous forests, which were dominated by *Picea* and *Abies*. This change probably included both an upslope and a downslope expansion of the conifer communities. Broadleaf trees such as *Quercus*, *Ulmus*, *Juglans* and *Acer* were probably present, but were reduced to minor elements in the lowland forests, the latter probably dominated by *Betula*. The increased importance of *Abies* and *Picea* suggests the occurrence of moist climates, if *Abies sachalinensis*, *Picea ajanensis* and *Picea glehnii*, which are present today, are the conifers represented by the pollen (Suslov 1961). Although the first two species require well-drained, mineral-rich soils, *Picea glehnii* needs a mesic substrate. The low percentages of *Pinus* s/g Haploxylon pollen suggest that the increased moisture was limited to the warm season. Razjigaeva *et al*. (2004) described a major climatic deterioration *c*. 3.2 to 2.6 cal. ka BP associated with the southward shift of mixed conifer–broadleaf forests and the dominance of *Picea* on most of Kunashir Island. Although the Glukhoye spectra reflect the increase in *Picea*, the timing (*c*. 2.3 to 1.1 cal. ka BP) is younger than documented in the sections. Such a difference probably reflects problems in the chronologies and related age models in both site types. A peak in Late Holocene cooling (*c*. 1.6 to 1.2 cal. ka BP), seen in the section data, was also noted in the Glukhoye record. However, the timing of the cool event differs (*c*. 2.3 to 1.1 cal. ka BP, again probably related to age models) and is not as intense as suggested in the sections.

The palynological spectra from PZ6 (*c*. 1.1 cal. ka BP to present), excepting *Pinus* s/g Haploxylon, suggest that modern vegetation was in place by *c*. 1.1 cal. ka BP, an age that approximates that noted by Razjigaeva *et al*. (2013) for the southern Kuril Islands. The increased presence of *Pinus pumila* in the middle of PZ6 suggests snowier conditions *c*. 0.8 to 0.5 cal. ka BP and is perhaps associated with Little Ice Age (LIA) climates. A LIA

cooling also has been noted in the section, but in the case of both site types, the dating is insufficient to be definitive.

Sections and lacustrine cores: reliability of palaeovegetation records from the Kuril Islands

Although analyses of lake and peat cores are now more common in areas of the SRFE (Bazarova *et al*. 2008; Lozhkin *et al*. 2010, 2021; Dirksen *et al*. 2013, 2015; Hammarlund *et al*. 2015; Hoff *et al*. 2015; Leipe *et al*. 2015), the current ideas about Holocene vegetation and climate change still rely heavily on data from sections. This is particularly true for the Kuril Islands. Palynological data extracted from sections usually represent differing depositional environments (e.g. soils, peats, lakes, alluvium) that can vary in their representation of local vs. regional vegetation (*sensu* Prentice 1988; see also Jacobson & Bradshaw, 1981). Furthermore, sections have a discontinuous depositional history, which complicates the formulation of reliable age models. Although lacustrine records are generally considered reliable sources for defining broader-scale patterns in the vegetation (Jacobson & Bradshaw 1981; Prentice 1988; Davis 2000), the coastal lakes in the Kuril Islands also have a complex depositional history (Fig. 7).

Despite these complications, some general conclusions can be drawn about pollen–vegetation and pollen deposition–vegetation relationships for the Kuril lacustrine records. A qualitative comparison of pollen spectra from surficial lake sediments to the modern vegetation showed that the lakes register variations in the major vegetation communities (i.e. the broadleaf forests of the southern Kurils, the transitional *Betula* forests of the central Kurils and the shrub tundra of the northern islands; Anderson & Lozhkin 2017). Korotky *et al*. (2000) and Razjigaeva *et al*. (2013) also noted that modern pollen samples from both lacustrine and non-lacustrine sediments reflect the main vegetation types of the Archipelago. However, these studies did not discuss any variations in the pollen spectra as related to differences in depositional setting, nor are brackish lagoons included in the modern data set. A visual inspection of stratigraphic boundaries based on palynological, diatom and lithological data from coastal lake cores in both the Kuril Islands and the SRFE mainland shows that times of change in the pollen data do not correspond to times when the depositional environment had altered (Anderson *et al*. 2015; Lozhkin *et al*. 2017, 2021). This simple comparison suggests that shifts in the pollen assemblages are the result of changes in vegetation and not in the depositional setting. In a more quantitative approach, Azuara *et al*. (2019) adapted the REVEALS model (Sugita 2007), which was initially applied to lakes, to evaluate pollen–vegetation relationships as recorded in coastal lagoons. They concluded that the model that had been developed to account for the dispersal and deposition of pollen, pollen source areas and estimation of regional vegetation in lakes is applicable to coastal lagoons. They also noted that changes to a basin's geometry did not affect any of the above parameters. The model, thus, provides additional support that shifts from a lagoon to a lake should not significantly impact the Kuril pollen records.

Another problem for interpreting the palaeovegetation of the Kuril Islands is the paucity and uneven spatial distribution of the sites. Although the modern samples suggest that the different site types record broadscale vegetation patterns, combining palynological data from lacustrine and sections indicates that the palaeorecords are not as straightforward (Fig. 7, Table 4; the material presented in Table 4 is adapted from Razjigaeva *et al*. 2013). The best-case scenario is that of Kunashir Island. Here the palaeovegetation changes described in the previous section indicate a general agreement in the sequence of vegetation types between the sections and the Glukhoye record, although there is some discrepancy in timing. The latter most likely reflects problems in chronologies from both site types. Comparisons of lacustrine and section reconstructions from Iturup Island, located to the north of Kunashir Island (Fig. 1A), and from the northern Kurils (Onekotan Island, sections; Paramushir Island, lake) show more variation (Table 4, Fig. 7). The Maloye Lake record from central Iturup Island indicates the initial presence of *Betula*–conifer forest (*c*. 8.2 to 7.4 cal. ka BP) followed by the establishment of *Betula–Quercus*–broadleaf forest (*c*. 7.4 to 6.1 cal. ka BP), which marks the Holocene thermal optimum (Lozhkin *et al*. 2017). In contrast, the sections show the presence of a mix of broadleaf–*Betula* forest and *Betula*–conifer forest between *c*. 8.1 and 5.4 cal. ka BP (Razjigaeva *et al*. 2013). The Maloye record suggests a gradual change in the vegetation as climate cooled with the modern vegetation established over the past 200–400 years. The sections indicate a more abrupt cooling with the presence of *Betula–Quercus* forests *c*. 5.4 to 4.3 cal. ka BP followed by *Betula* forest with a minor component of *Quercus* and the establishment of modern vegetation at *c*. 1.4 cal. ka BP. The Holocene optimum is placed at *c*. 6.8 to 5.7 cal. ka BP. Even greater differences are seen in the Onekotan and Paramushir records, where the interval of *Pinus pumila–Duschekia* shrub tundra differs between *c*. 9.2 and 8.6 cal. ka BP in the sections (note: 9.2 cal. ka BP represents the bottom of the section data) and from *c*. 9.1 to 6.5 cal. ka BP in the lakes. Modern vegetation established *c*. 3.2 cal. ka BP (section) and *c*. 5.5 cal. ka BP (lake). The section data that show major discontinuities related to volcanic deposits are found only in the sections.

Conclusions that can be drawn from the above comparisons are limited by the small number of lakes and the uneven numbers of sections from any island. However, some tentative inferences can be made. For

Table 4. Summary of Middle to Late Holocene vegetation, Kuril Islands, from section data.

Location	Age (cal. ka BP)	Vegetation description
Southern Kurils		
Kunashir Island	8.9–7.5	Mixed *Betula* forest and meadows
	7.5–5.7	Cool temperate *Quercus*–broadleaf (*Juglans*, *Ulmus*, *Tilia*, *Fraxinus*) forest with conifers (*Picea*, *Abies*)
	5.7–2.3	Mixed *Quercus*–broadleaf forest with conifers
	2.3–0.7	Mixed conifer–*Quercus* broadleaf forest with decrease in broadleaf species and increase in tree *Betula*, meadows and bogs as compared with the previous interval
	0.7–0	Modern mix of *Quercus* broadleaf and conifer forest
Central Kurils		
Rasshua Island	9.1–8.1	Mixed shrub *Betula* tundra and graminoid meadows
	8.1–7.6	Graminoid–forb meadows and bogs
	7.6–6.8	Mixed *Pinus pumila–Duschekia* shrub Tundra and forb meadows
	6.8–5.5	*Duschekia* shrub tundra and graminoid –forb meadows
	5.5–4.5	Heaths with *Pinus pumila–Duschekia* thickets
		Hiatus
	4.5–3.1	Mixed *Pinus pumila–Duschekia* shrub
	3.1–1.9	tundra and graminoid–forb meadows
		Hiatus
	1.9–1.4	Modern *Pinus pumila–Duschekia* shrub
	1.4–0	tundra; decrease in *Pinus pumila* and shrub *Betula* as compared with the previous interval
Northern Kurils		
Onekotan Island	9.5–8.6	Heath with scattered shrub thickets of *Betula* and *Duschekia*
	8.6–8.3	Graminoid–forb meadows, succession
	?	of pioneering communities following eruption of Tao-Rusyr volcano at *c* 8.3 cal. ka BP
	5.6–3.2	*Pinus pumila* shrub tundra with greater boggy areas as compared with the previous interval
	3.2–2.3	*Pinus pumila–Duschekia* shrub tundra
	2.3–0	Modern mix of *Pinus pumila–Duschekia* shrub tundra, graminoid–forb meadows and wetlands

example, the closest similarity in records from the different site types is from Kunashir Island, where the number of analysed sections is the greatest (Razjigaeva *et al*. 2013). The Onekoton–Paramushir comparison clearly shows that the section data are more sensitive to volcanic activity on the landscape. In contrast the lacustrine cores, while containing dispersed tephra, show no discrete ash layers. Thus, the differences in the lake and section records seem to have more to do with the number of section sites per island, the number of radiocarbon dates per site and the development of site age-models than they do with pollen representation issues related to the depositional environment. Although data from different site types can be combined with some caution for the southern Kurils, insufficient numbers of sites exist at this time to provide a definitive vegetation or climate history for the Middle to Late Holocene of the central and northern Kuril Archipelago.

Implications of the lacustrine records from the Kuril Islands for a section-based model of Holocene climate change

Korotky *et al*. (1996, 2000) proposed a conceptual model of Holocene climate fluctuations based on lithological and palaeobotanical data from sections in both the SRFE mainland and the Kuril Islands, the latter area relying primarily on data from Kunashir Island. They linked regional changes in climate to sea level (warmer climates and higher sea levels; cooler climates and lower sea levels). Times of regression/cool climate were reflected as periods of dune formation in the coastal sections. Transgressions/warm climate were marked by indicators of shallow straits (e.g. marine molluscs and brackish to saline diatom assemblages) within the low-lying isthmuses that characterized the southern Kuril Islands and the presence of elevated marine terraces along the coasts. Rising sea level also resulted in large amounts of detrital material being deposited in the coastal zones, in some areas causing the development of coastal lakes. According to this model, the Middle and Late Holocene climate fluctuations were characterized by three intervals of dune formation and cool climates (*c*. 5.4 to 5.2 cal. ka BP, *c*. 1.6 to 1.2 cal. ka BP, LIA), a major warm/transgressive period (*c*. 7.4 to 6.8 cal. ka BP; +2.5 to 3.0 m p.s.l.), a second transgression with conditions only slightly cooler than during the HTM (*c*. 4.5 to 3.5 cal. ka BP; +1.25 to 2.5 m p.s.l.), and two occurrences of more modest warming/transgressions (*c*. 3.1 to 2.7 and *c*. 1.2 to 0.7 cal. ka BP). As their model relies heavily on changes in coastal conditions, the lake cores, although few, add further information with which to evaluate the proposed palaeoclimate scheme.

Comparisons of lithological and palynological data from present-day lakes in coastal areas of Iturup and Paramushir Island (Anderson *et al*. 2015; Lozhkin *et al*. 2017) to the Glukhoye record do not support the linkage of region-wide sea level fluctuations and climate change as proposed by the Korotky *et al*. model (Fig. 7). Although the lacustrine records do indicate that sea levels were higher during the Middle Holocene (i.e. presence of brackish lagoons), the timing of these high stands varies among the sites (Glukhoye Lake high sea levels present by at least *c*. 8.2 and persisting to *c*. 4.3 cal. ka BP; Maloye Lake present by at least *c*. 8.2 cal. ka BP and persisting to *c*. 7.1 cal. ka BP; Pernatoye Lake *c*. 10.1 to 6.0 cal. ka BP). Furthermore, none of these records indicate additional high stands (i.e. re-establishment of lagoons) during the Late Holocene. Each of the lake

records include discrete sand layers, which we have suggested in previous publications (Anderson *et al.* 2015; Lozhkin *et al.* 2017), might reflect the development of coastal dunes during times of regression/cool climate (Fig. 7). Maloye and Pernatoye lakes include four sand layers, whereas Glukhoye Lake has only two. All three records have a sand deposit *c.* 4000 cal. ka BP, a time of transgression in the palaeoclimate scheme. Only Maloye and Pernatoye lakes show a *c.* 1000 cal. ka BP event, which is also proposed as a cool interval in the model. Temporal offsets within and between lacustrine and section data can be attributed to the uncertainties in the age models. Nonetheless, the inconsistencies in the numbers of 'cool' events among the lacustrine cores and between these records and the palaeoclimate model suggest that the sand layers in the lakes are not related to cool conditions associated with sea regression and coastal dune formation. It seems more likely that the sandy deposits reflect local processes, such as erosion of sandy deposits along inflowing streams or from embankments bordering the basin.

Palynological data from the lacustrine sites indicate a gradual cooling from a Holocene thermal maximum, again in contrast to the varying climates suggested by Korotky *et al.* (1996, 2000) for the Middle and Late Holocene. The interval of maximum warmth in all the lacustrine sites partially overlaps the *c.* 7.4 to 6.8 cal. ka BP age for the HTM as proposed in the model for the entire Archipelago, but the lakes show greater temporal variability (Glukhoye Lake *c.* 8.0 to 6.5 cal. ka BP; Maloye Lake *c.* 7.0 to 6.1 cal. ka BP; Pernatoye Lake *c.* 9.0 to 6.6 cal. ka BP). Here again some temporal offset for the Holocene optimum probably represents the quality of chronological control. However, a Late Holocene pattern of gradual cooling (lakes) and one with fluctuations between relatively cool and warm conditions (sections) is difficult to reconcile based solely on dating.

Conclusions

Previous results from lacustrine cores from Iturup and Paramushir Islands (Lozhkin *et al.* 2010, 2017; Anderson *et al.* 2015) and from a coastal lake on the mainland (Lozhkin *et al.* 2021) indicated that changes in palynological assemblages were independent of shifts in depositional environments, even in cases of significant differences, such as the shift from marine lagoons to freshwater lakes. The Glukhoye record also confirms these findings and underscores the usefulness of the coastal lacustrine records for palaeovegetation interpretations.

Comparisons of palaeovegetation changes based on the lacustrine cores (Fig. 7) vs. the composite sections (Table 4) indicate that the greatest similarity between the two data types occurs in the Kunashir records. Kunashir is also the island with the largest number of radiocarbon-dated sections, suggesting that: (i) there is an extra local vegetation signal that can be gleaned from the sections; (ii) the ability to understand the regional over the local vegetation history improves as the number of analysed sections increases; and (iii) at least qualitative palaeoclimate trends can be inferred for well-sampled islands. However, the timing of the vegetation changes differs between the two data types, reflecting the challenge for developing accurate age models in either discontinuous records or records with significant changes in depositional environments.

In previous publications, Lozhkin and colleagues (Anderson *et al.* 2015; Lozhkin *et al.* 2017, 2021) noted that multiple changes in sea level, which had been proposed by Korotky *et al.* (1996, 2000) as correlating to Middle and Late Holocene climate fluctuations, were not supported by the diatoms or lithology, nor the geochemistry of the coastal lake records. This conclusion also holds true for Glukhoye Lake. In the palaeoclimate model proposed, periods of intense dune formation corresponded to intervals of relative cooling *c.* 5.4 to 5.2 and *c.* 1.6 to 1.2 cal. ka BP, and during the LIA. Lozhkin and colleagues considered that the sand layers preserved in the lake cores were possible indicators of coastal dune formation and/or greater aeolian input associated with lowered sea levels and a broader exposure of shelf sediments. Although Maloye (Iturup Island) and Pernatoye (Paramushir Island) lakes include Middle to Late Holocene sand layers, the timing and numbers do not correspond to episodes of sea level regression as proposed in the model. The Glukhoye core has fewer and thinner sand layers as compared with the other lakes, and the ages of the Glukhoye sands do not coincide with the proposed times of lowered sea levels. Rather the histories of the lake basins seem to be related to local coastal dynamics that are independent of climate change.

In addition to the basin history, the palynological data from the lake records indicate gradual changes in vegetation and climate from an interval of maximum warmth to modern conditions. This pattern contrasts with the Korotky *et al.* (1996, 2000) model, where the Middle and Late Holocene were punctuated by intervals of warmer and cooler climates. Although the palaeovegetation interpretations of palynological data in both lakes and sections indicate a thermal optimum during the Middle Holocene, this interval varies from *c.* 7.5 to 5.7 cal. ka BP (for the entire Kuril Islands based on sections; Razjigaeva *et al.* 2013), from *c.* 8.0 to 6.5 cal. ka BP (Kunashir Island, lake data; this paper), from *c.* 7.0 to 6.1 cal. ka BP (Iturup Island, lake data; Lozhkin *et al.* 2017) and from *c.* 9.0 to 6.6 cal. ka BP (Paramushir Island, lake data; Anderson *et al.* 2015). Such variation again speaks to the difficulties of age modelling, which may be the more important obstacle for documenting and understanding causes of the Archipelago's palaeoenvironmental history than are the

influences of sea levels or of subregional factors, such as volcanic eruptions or tsunamis.

Acknowledgements. – Primary support for this research was provided by the National Science Foundation (ARC-0508109) and the Russian Foundation for Fundamental Research (project no. 19-05-00477). Additional support was provided by the UW Center for Study of Demography and Ecology under support from a Eunice Kennedy Shriver National Institute of Child Health and Human Development research infrastructure grant, R24 HD042828 and by the Sakhalin Regional Museum (Yuzhno–Sakhalinsk, Russia). We appreciate help and information provided by Natalya Eremenko, botanist for the South Kuril Island Nature Preserve, and thank the Preserve for allowing us access for coring. We also thank Julia Korzun and Valeriya Tsygankova for help in manuscript preparation and two unnamed reviewers for their helpful comments on an earlier version of the manuscript. Original data will be made available upon request from the authors.

Author contributions. – AL and PA were responsible for palynological analysis, writing of the original draft, field work and funding acquisition. MC was responsible for diatom analysis and writing of the original draft. BF was responsible for the geochemical analysis and writing of the original draft. PM was involved in field work and funding acquisition.

References

Alekseeva, L. M. 1983: *Flora of Kunashiri Island (Vascular Plants)*. 129 pp. Far East Scientific Center of the USSR Academy of Sciences, Vladivostok (in Russian).

Alexsandrova, A. N. 1971: Some questions of Quaternary stratigraphy of Iturup. *Reports of the Sakhalin Department of the USSR Geographical Society 2*, 74–81 (in Russian).

Alhonen, P., Heino, A. & Tynni, R. 1984: Über Vorkommen und Bedeutung von *Terpsinoe americana* (Bail.) Ralfs in den Ablagerungen des Litorinameeres. *Bulletin of the Geological Society of Finland 56*, 117–133.

Anderson, P. M. & Lozhkin, A. V. 2017: Modern pollen rain from lake sediments of the Kuril Islands. *Vestnik 1*, 3–13.

Anderson, P. M., Lozhkin, A. V., Minyuk, P. S., Pakhomov, A. Y. & Solomatkina, T. B. 2009: Pollen record and sediment ages from lakes of Kunashir and Iturup islands (Southern Kurils). *In* Baklanov, P. Ya. (Chairman of Editorial Board): *Environment Development of East Asia in the Pleistocene-Holocene (Boundaries, Factors, Stages of Human Mastering)*, 13-16. *Proceedings of International Scientific Conference, September 14-18, 2009*. Dalnauka, Vladivostok.

Anderson, P. M., Minyuk, P. S., Lozhkin, A. V., Cherepanova, M., Borkhodoev, V. & Finney, B. P. 2015: Multiproxy record of Holocene environmental changes from the northern Kuril Islands (Russian Far East). *Journal of Paleolimnology 54*, 379–393.

Andreev, V. N. 1980: Some data about lichen-free tundra. *In* Andreev, V. N. (ed.): *Vegetation and Soils of Subarctic Tundra*, 201–205. Siberian Branch Yakutia Subdivision Biological Institute USSR Academy of Sciences, Novosibirsk (in Russian).

Avramenko, A. S., Cherepanova, M. V., Pushkar, V. S. & Yarusova, S. B. 2015: Diatom characteristics of the Far East siliceous organogenic deposits. *Russian Geology and Geophysics 56*, 947–958.

Azuara, J., Mazier, F., Lebreton, V., Sugita, S., Viovy, N. & Combourieu-Nebout, N. 2019: Extending the applicability of the REVEALS model for pollen-based vegetation reconstructions to coastal lagoons. *The Holocene 29*, 1109–1112.

Barinova, S. S., Medvedeva, L. A. & Anisimova, O. V. 2006: *Diversity of Algal Indicators in Environmental Assessment*. 498 pp. Pilies Studio, Tel Aviv (in Russian).

Barkalov, V. Y. 2009: *Flora of the Kuril Islands*. 135 pp. Dalnauka, Vladivostok (in Russian).

Bazarova, V. B., Klimin, M. A., Mokhova, L. M. & Orlova, L. A. 2008: New pollen records of Late Pleistocene and Holocene changes of environment and climate in the lower Amur River basin, NE Asia. *Quaternary International 179*, 9–19.

Blaauw, M. & Christen, J. A. 2011: *Bacon Manual – v. 2.2*. http://www.chron.qub.ac.uk/blaauw/bacon.html.

Blaauw, M. & Heegaard, E. 2012: Estimation of age-depth relationships. *In* Birks, H. J. B., Lotter, A. F., Juggins, S. & Smol, J. P. (eds.): *Tracking Environmental Change Using Lake Sediments: Data Handling and Numerical Techniques*, 379–413. Springer, Amsterdam.

Bourgeois, J., Pinegina, T. K. & Zaretskaia, N. 2006: Holocene tsunamis in the southwestern Bering Sea, Russian Far East, and their tectonic implications. *Geological Society of America 118*, 449–463.

Czerepanov, S. K. 1995: *Vascular Plants of Russia and Adjacent States (the Former USSR)*. 516 pp. Cambridge University Press, Cambridge.

Davis, M. B. 2000: Palynology after Y2K – Understanding the source area of pollen in sediments. *Annual Review of Earth and Planetary Sciences 28*, 1–18.

Ding, Y. H. & Chan, C. L. 2005: The East Asian summer monsoon: a review. *Meteorology and Atmospheric Physics 89*, 117–142.

Dirksen, V., Dirksen, O., van den Bogaard, C. & Diekmann, B. 2015: Holocene pollen record from Lake Sokoch, interior Kamchatka (Russia), and its paleobotanical and paleoclimatic record. *Global and Planetary Change 134*, 129–141.

Dirksen, V., Dirksen, O. & Diekmann, B. 2013: Holocene vegetation dynamics and climate change in Kamchatka Peninsula, Russian Far East. *Review of Palaeobotany and Palynology 190*, 48–65.

Donar, C. M., Neely, R. K. & Stoermer, E. F. 1996: Diatom succession in an urban reservoir system. *Journal of Paleolimnology 15*, 237–243.

Ganzei, K. 2011: *Landscape Forming Factors of Kurile Islands (North-Western Pacific)*. 94 pp. Lambert Academic Publishing, Saarbruken.

Gibson, C. E., Anderson, N. J. & Haworth, E. Y. 2003: *Aulacoseira subarctica*: taxonomy, physiology, ecology and palaeoecology. *European Journal of Phycology 38*, 83–101.

Gleser, Z. I., Jousé, A. P., Makarova, I. V., Proshkina-Lavrenko, A. I. & Sheshukova-Poretskaya, V. S. (eds.) 1974: *Diatoms of the USSR: Fossil and Modern*. 403 pp. Nauka, Leningrad (in Russian).

Goldfarb, S. I. 2014: *Geographical Encyclopedia of the Kuril Islands*. 254 pp. Publishing House Komsomolskaya Pravda, Moscow (in Russian).

Gorbarenko, S. A., Artemova, A. V., Goldberg, E. L. & Vasilenko, Y. P. 2014: The response of the Okhotsk Sea environment to the orbital-millennium global climate changes during the Last Glacial Maximum, deglaciation and Holocene. *Global and Planetary Change 116*, 76–90.

Gorbarenko, S. A., Southon, J. R., Keigwin, L. D., Cherepanova, M. V. & Gvozdeva, I. G. 2004: Late Pleistocene-Holocene oceanographic variability in the Okhotsk Sea: lithological and paleontological evidence. *Palaeogeography, Palaeoclimatology, Palaeoecology 209*, 281–301.

Hammarlund, D., Klimaschewski, A., St. Amour, N. A., Andrén, E., Self, A. E., Solovieva, N., Andreev, A. A., Barnekow, L. & Edwards, T. W. D. 2015: Late Holocene expansion of Siberian dwarf pine (*Pinus pumila*) in Kamchatka in response to increased snow cover as inferred from lacustrine oxygen-isotope records. *Global and Planetary Change 134*, 91–100.

Harada, N., Akagon, N., Uchida, M. & Murayama, M. 2004: Northward and southward migrations of frontal zones during the last 40 kyr in the Kuroshio-Oyashio transition area. *Geochemistry, Geophysics, Geosystems 5*, Q09004, https://doi.org/10.1029/2004GC00740.

Harada, N., Katsuki, K., Nakagawa, M., Matsumoto, A., Seki, O., Addison, J. A. & Finney, B. P. 2014: Holocene sea surface temperature and sea ice extent in the Okhotsk and Bering Seas. *Progress in Oceanography 126*, 242–253.

Hoff, U., Biskaborn, B. K., Dirksen, V. G., Dirksen, O., Kuhn, G., Meyer, H., Nazarova, L., Roth, L. & Diekmann, B. 2015: Holocene environment of Central Kamchatka, Russia: Implications from a multi-proxy record of Two-Yurts Lake. *Global and Planetary Change 134*, 101–117.

Inagaki, M., Yamamoto, M., Igarashi, Y. & Ikehara, K. 2009: Biomarker records from core GH02-1030 off Tokachi in the Northwestern Pacific over the last 23,000 years: Environmental changes during the last deglaciation. *Journal of Oceanography 65*, 847–858.

Ivanova, G. P. (ed.) 1990: *Scientific and Applied Reference Book on the Climate of the USSR. Issue 34. Sakhalin Region*. 351 pp. Gidrometheoizdat, Leningrad (in Russian).

Jacobson Jr, G. I. & Bradshaw, R. H. W. 1981: The selection of sites for paleovegetational studies. *Quaternary Research 16*, 80–96.

Jouze, A. P. 1962: *Stratigraphical and Paleogeographical Investigations in the North-Western Part of the Pacific Ocean*. 258 pp. USSR Academy of Sciences Publication, Moscow (in Russian).

Juracek, K. E. 2003: Sediment Deposition and Occurrence of Selected Nutrients, Other Chemical Constituents, and Diatoms in Bottom Sediment, Perry Lake, Northeast Kansas, 1969–2001. *U.S. Geological Survey Water-Resources Investigations Report 03–4025*. 56 pp.

Kirilova, E. P., Cremer, H., Heiri, O. & Lotter, A. F. 2010: Eutrophication of moderately deep Dutch lakes during the past century: flaws in the expectations of water management? *Hydrobiologia 637*, 157–171.

Korotky, A. M. 2002: Palynological characteristics and radiocarbon data of late Quaternary deposits of the Russian Far East (lower Amur valley, Primor'ye, Sakhalin Island, Kuril Islands). *In* Anderson, P. M. & Lozhkin, A. V. (eds.): *Late Quaternary Vegetation and Climate of Siberia and the Russian Far East (Palynological and Radiocarbon Database)*, 257–265. NOAA Paleoclimatology and North East Science Center, Magadan.

Korotky, A. M., Pletnev, S. P., Pushkar, V. S., Grebennikova, T. A., Razjigaeva, N. G., Sakhbgareeva, E. D. & Mokhova, L. M. 1988: *Evolution Environment of South Far East (Late Pleistocene and Holocene)*. 240 pp. Nauka, Moscow (in Russian).

Korotky, A. M., Razjigaeva, N. G., Grebennikova, T. A., Ganzey, L. A., Bazarova, V. B., Sulerzhitsky, L. D. & Lutaenko, K. A. 2000: Middle- and late-Holocene environments and vegetation history of Kunashir Island, Kurile Islands, northwestern Pacific. *The Holocene 10*, 311–331.

Korotky, A. M., Razjigaeva, N. G., Mokhova, L. M., Ganzey, L. A., Grebennikova, T. A. & Bazarova, V. B. 1996: Coastal dunes as an indicator of period of global climatic deterioration (Kunashir Island, Kurils). *Geology of the Pacific Ocean 13*, 73–84.

Korotky, A. M., Volkov, V. G., Grebennikova, T. A., Razjigaeva, N. G., Pushkar, V. S., Ganzei, L. A. & Mokhova, L. M. 2005: Far East. *In* Velichko, A. A. (ed.): *Cenozoic Climate and Environmental Changes in Russia*, 121–137. *Geological Society of America Special Papers 382*.

Kotlyakov, V. M., Baklanov, P. Y. & Komedchikov, N. N. (eds.) 2009: *Atlas of the Kuril Islands*. 515 pp. Institute of Geography, Russian Academy of Sciences and Russian Academy of Sciences, Far East Branch, Pacific Institute of Geography, Moscow and Vladivostok (in Russian).

Kozhevnikov, Y. P. 1981: Ecology-floristic changes in the middle part of the Anadyr River basin. *In* Mazurenko, M. T. (ed.): *Biology of Plants and Flora of North of Far East*, 65–78. Institute of Biological Problems of the North, Far East Branch USSR Academy of Science, Vladivostok (in Russian).

Leipe, C., Nakagawa, T., Gotanda, K., Muller, S. & Tarasov, P. E. 2015: Late Quaternary vegetation and climate dynamics at the northern limit of the East Asian summer monsoon and its regional and global-scale controls. *Quaternary Science Reviews 116*, 57–71.

Lozhkin, A. V., Anderson, P. M., Brown, T. A., Grebennikova, T. A., Korzun, J. A. & Tsygankova, V. I. 2021: Lake development in coastal areas of Primor'ye: Implications for Holocene climate and vegetation patterns in southeastern regions of the Russian Far East. *Boreas 50*. https://doi.org/10.1111/bor.12.

Lozhkin, A. V., Anderson, P. M., Goryachev, N. A., Minyuk, P. S., Pakhomov, A. Y., Solomatkina, T. B. & Cherepanova, M. V. 2010: First Lake Record of Holocene Climate and Vegetation Change from the Northern Kuril Islands. *Doklady Academii Nauk 430*, 541–543. (in Russian).

Lozhkin, A. V., Cherepanova, M. V., Anderson, P. M., Minyuk, P. S., Finney, B., Pakhomov, A., Brown, T. A., Korzun, J. A. & Tsigankova, V. I. 2020: Late Holocene history of Tokotan Lake (Kuril Archipelago, Russian Far East): The use of lacustrine records for paleoclimatic reconstructions from geologically dynamic settings. *Quaternary International 553*, 104–117.

Lozhkin, A., Minyuk, P., Cherepanova, M., Anderson, P. & Finney, B. 2017: Holocene environments of Iturup Island, southern Kuril Archipelago, Russian Far East. *Quaternary Research 88*, 23–38.

Lyaschevskaya, M. S. & Ganzei, K. S. 2011: Environmental development of central part of the Iturup Island at Middle-Late Holocene (Kuril Islands). *Bulletin of KRAESC Earth Sciences Series 17*, 35–45.

Martyn, D. 1992. *Climates of the World. Developments in Atmospheric Science 18*. 416 pp. Elsevier, Amsterdam.

Mock, C. J. 2002: Regional climates of Russia. *In* Anderson, P. M. & Lozhkin, A. V. (eds.): *Late Quaternary Vegetation and Climate of Siberia and the Russian Far East (Palynological and Radiocarbon Database)*, 17–26. NOAA Paleoclimate Program & North East Science Center, Magadan.

Okazakia, Y., Takahashib, K., Katsukib, K., Onob, A., Horib, J., Sakamotoc, T., Shibatae, Y., Ikeharaf, M. & Aokig, K. 2005: Late Quaternary paleoceanographic changes in the southwestern Okhotsk Sea: Evidence from geochemical, radiolarian, and diatom records. *Deep Sea Research II 52*, 2332–2350.

PALE 1994: *Research Protocols for PALE: Paleoclimates of Arctic Lakes and Estuaries*. 53 pp. PAGES Workshop Report Series, Bern.

Pietsch, T. W., Bogatov, V. V., Amaoka, K., Zhuravlev, Y. N., Barkalov, V. Y., Gage, S., Takahashi, H., Lelej, A. S., Storzhenko, Y. N., Minakawa, N., Bennett, D. J., Anderson, T. R., Ohara, M., Prozorova, L. A., Kuwahasara, Y., Kholin, S. K., Yabe, M., Stevenson, D. E. & MacDonald, E. L. 2003: Biodiversity and biography of the islands of the Kuril Archipelago. *Journal of Biogeography 30*, 1297–1310.

Prentice, I. C. 1988: Records of vegetation in time and space: the principles of pollen analysis. *In* Huntley, B. & Webb T. (eds.): *Handbook of Vegetation Science Vegetation History*, 17–42. Kluwer Academic Publishers, Dordrecht.

Pryalukhina, A. F. 1961: Materials of South Kurile Islands stratigraphy. *Reports of the Sakhalin Complex Scientific Research Institute USSR Academy of Science 10*, 3–13. (in Russian).

Razjigaeva, N. G., Ganzei, L. A., Grebennikova, T. A., Belyanina, N. I., Mokhova, L. M., Arslanov, K. A. & Chernov, S. B. 2013: Holocene climatic changes and vegetation development in the Kuril Islands. *Quaternary International 290–291*, 126–138.

Razjigaeva, N. G., Ganzei, L. A., Grebennikova, T. A., Kharlamov, A. A., Arslanov, K. A., Kaistrenko, V. M., Gorbunov, A. O. & Petrov, A. Y. 2017: The problem of paleoreconstruction of paleotsunami in the South Kuril Islands. *Russian Pacific Geology 36*, 39–51. (in Russian).

Razjigaeva, N. G., Ganzei, L. A., Mokhova, L. M. & Pshenichnikova, N. F. 2011b: Meadow landscapes of the Southern Kuriles: origin, age and development. *Geography and Natural Resources 3*, 96–104.

Razjigaeva, N. G., Ganzey, L. A., Arslanov, K. A., Grebennikova, T. A., Belyanina, N. I. & Mokhova, L. M. 2011a: Paleoenvironments of Kuril Islands in Late Pleistocene-Holocene: Climatic changes and volcanic eruptions. *Quaternary International 237*, 4–14.

Razjigaeva, N. G., Ganzey, L. A., Belynina, N. I., Grebennikova, T. A. & Ganzey, K. S. 2008: Paleoenvironments and landscape history of the minor Kuril Islands since the late glacial. *Quaternary International 179*, 83–89.

Razjigaeva, N. G., Grebennikova, T. A., Ganzey, L. A., Mokhova, L. M. & Bazarova, V. B. 2004: The role of global and local factors in determining the middle to late Holocene environmental history of the South Kurile and Komandar Islands, northwestern Pacific. *Palaeogeography, Palaeoclimatology, Palaeoecology 209*, 313–333.

Razjigaeva, N. G., Korotky, A. M., Grebennikova, T. A., Ganzey, L. A., Mokhova, L. M., Bazarova, V. B., Sulerzhitsky, L. D. & Lutaenko, K. A. 2002: Holocene climatic changes and environmental history of Iturup Island, Kurile Islands, northwestern Pacific. *The Holocene 12*, 469–480.

Reimer, P. J., Bard, E., Bayliss, A., Beck, J. W., Blackwell, P. G., Bronk Ramsey, C., Buck, C. E., Cheng, H., Edwards, R. I., Friedrich, M., Grootes, P. M., Guilderson, T. P., Halidasson, H., Hajdas, I., Hatté, C., Heaton, T. J., Hoffman, D. I., Hogg, A. G., Hughen, K. A., Kaiser, K. F., Kromer, B., Manning, S. W., Niu, M., Reimer, R. W., Richards, D. A., Scott, E. M., Southon, J. R., Staff, R. A., Turney, C. A. & van der Plicht, J. 2013: IntCal13 and marine13 radiocarbon age calibration curves 0–50,000 years cal BP. *Radiocarbon 55*, 1869–1887.

Sato, H., Kumano, S., Maeda, Y., Nakamura, T. & Matsuda, I. 1998: The Holocene development of Kushu Lake on Rebun Island in Hokkaido, Japan. *Journal of Paleolimnology 20*, 57–69.

Sato, H., Maeda, Y. & Kumano, S. 1983: Diatom assemblages and Holocene sea level changes at the Tamatsu site in Kobe, western Japan. *The Quaternary Research (Japanese Association for Quaternary Research) 22*, 77–90.

Stuiver, M., Reimer, P. J. & Reimer, R. W. 2020: *CALIB 8.2* (WWW program) at http://calib.org. Accessed 20/6/2020.

Sugita, S. 2007: Theory of quantitative reconstruction of vegetation I: pollen from large sites REVEALS regional vegetation composition. *The Holocene 17*, 229–241.

Suslov, S. P. 1961: *Physical Geography of Asiatic Russia*. 594 pp. W.H. Freeman and Co, San Francisco.

Urusov, V. M. & Chipizubova, M. N. 2000: *Vegetation of Kuril Islands Questions of Dynamics and Origin*. 303 pp. Russian Academy of Sciences, Far East Branch, Vladivostok (in Russian).

Vorobiev, D. P. 1963: *Vegetation of the Kurile Islands*. 92 pp. USSR Academy of Sciences Press, Moscow (in Russian).

Walker, M., Head, M. J., Lowe, J., Berkelhammer, M., Bjorck, S., Cheng, H., Cwynar, L. C., Fisger, D., Gkinis, V., Long, A., Newnham, R., Rasmussen, S. O. & Weiss, H. 2019: Subdividing the Holocene Series/Epoch: formalization of stages/ages and subseries/subepochs, and designation of GSSPs and auxiliary stratotypes. *Journal of Quaternary Science 34*, 173–186.

Wright, H. E., Mann, D. H. & Glaser, P. H. 1984: Piston corers for peat and lake sediments. *Ecology 65*, 657–659.

Supporting Information

Additional Supporting Information may be found in the online version of this article at http://www.boreas.dk.

Fig. S1. Age–depth plot of calibrated ages for Glukhoye Lake.

Table S1. Dominant and common diatoms, Glukhoye Lake.